DOCUMENT CONTROL DATA - R&D
(Security classification of title, body of abstract and indexing annotation must be entered when the overall report is classified)

1. ORIGINATING ACTIVITY (Corporate author)	2a. REPORT SECURITY CLASSIFICATION
University of Dayton Research Institute Dayton, Ohio 45409	Unclassified
	2b. GROUP

3. REPORT TITLE

RESEARCH ON RARE EARTH-COBALT ALLOYS AND COMPOUNDS

4. DESCRIPTIVE NOTES (Type of report and inclusive dates)

5. AUTHOR(S) (Last name, first name, initial)

Jacques Schweizer

6. REPORT DATE	7a. TOTAL NO. OF PAGES	7b. NO. OF REFS
April 1972	59	26

8a. CONTRACT OR GRANT NO.	9a. ORIGINATOR'S REPORT NUMBER(S)
F33615-70-C-1625	
b. PROJECT NO.	UDRI-TR-72-27
7371	
c.	9b. OTHER REPORT NO(S) (Any other numbers that may be assigned this report)
Task No. 73103	AFML-TR-72-82
d.	

10. AVAILABILITY/LIMITATION NOTICES

Approved for Public Release - Distribution Unlimited

11. SUPPLEMENTARY NOTES	12. SPONSORING MILITARY ACTIVITY
	Air Force Materials Laboratory Wright-Patterson AFB, Ohio 45433

13. ABSTRACT

This report contains a collection of six papers dealing with some magnetic properties of rare earth-cobalt alloys and the crystalline and magnetic structures of some rare earth-cobalt intermetallic phases.

The variation of coercivity as a function of the temperature of annealing or sintering is reported for compacts of a single-phase $PrCo_5$ powder and also for a mixture of $PrCo_5$ with an additive richer in praseodymium.

A previously unidentified thermal event observed in some praseodymium-cobalt alloys is shown to be the peritectic reaction temperature of a new phase, Pr_5Co_{19}. The structures of the two crystallographic modifications of Pr_5Co_{19} are given.

The crystal structures of two previously unreported phases, $Pr_2Co_{1.7}$ and $Nd_2Co_{1.7}$ are given. It is shown that the phase designated as La_xCo in earlier work is actually $La_2Co_{1.7}$ and isostructural to the praseodymium and neodymium phases.

The magnetic structures of the compound $Pr_2Co_{1.7}$ and $Nd_2Co_{1.7}$ have been determined by neutron diffraction experiments conducted at room temperature and helium temperatures. Results of these experiments are presented.

A relatively simple technique for determining the easy axis of magnetization in a material with a large magnetocrystalline anisotropy by means of x-ray diffraction is described. The easy magnetic axes of most of the known R_2Co_{17} and R_2Fe_{17} phases, utilizing this technique, are reported.

The crystal structure of $Ho_{12}Co_7$ is reported. It is shown that this phase corresponds to the phase labeled Ho_xCo in the Ho-Co phase diagram.

DD FORM 1473
1 JAN 64

NOTICES

When Government drawings, specifications, or other data are used for and purpose other than in connection with a definitely related Government procurement operation, the United States Government thereby incurs no responsibility nor any obligation whatsoever; and the fact that the Government may have formulated, furnished, or in any way supplied the said drawings, specifications, or other data, is not to be regarded by implication or otherwise as in any manner licensing the holder or any other person or corporation, or conveying any rights or permission to manufacture, use, or sell any patented invention that may in any way be related thereto.

14		LINK A		LINK B		LINK C	
	KEY WORDS	ROLE	WT	ROLE	WT	ROLE	WT
rare earth alloys							
rare earth compounds							
magnetic properties							
crystal structures							
magnetic structures							

INSTRUCTIONS

1. ORIGINATING ACTIVITY: Enter the name and address of the contractor, subcontractor, grantee, Department of Defense activity or other organization (*corporate author*) issuing the report.

2a. REPORT SECURITY CLASSIFICATION: Enter the overall security classification of the report. Indicate whether "Restricted Data" is included. Marking is to be in accordance with appropriate security regulations.

2b. GROUP: Automatic downgrading is specified in DoD Directive 5200.10 and Armed Forces Industrial Manual. Enter the group number. Also, when applicable, show that optional markings have been used for Group 3 and Group 4 as authorized.

3. REPORT TITLE: Enter the complete report title in all capital letters. Titles in all cases should be unclassified. If a meaningful title cannot be selected without classification, show title classification in all capitals in parenthesis immediately following the title.

4. DESCRIPTIVE NOTES: If appropriate, enter the type of report, e.g., interim, progress, summary, annual, or final. Give the inclusive dates when a specific reporting period is covered.

5. AUTHOR(S): Enter the name(s) of author(s) as shown on or in the report. Enter last name, first name, middle initial. If military, show rank and branch of service. The name of the principal author is an absolute minimum requirement.

6. REPORT DATE: Enter the date of the report as day, month, year, or month, year. If more than one date appears on the report, use date of publication.

7a. TOTAL NUMBER OF PAGES: The total page count should follow normal pagination procedures, i.e., enter the number of pages containing information.

7b. NUMBER OF REFERENCES: Enter the total number of references cited in the report.

8a. CONTRACT OR GRANT NUMBER: If appropriate, enter the applicable number of the contract or grant under which the report was written.

8b, 8c, & 8d. PROJECT NUMBER: Enter the appropriate military department identification, such as project number, subproject number, system numbers, task number, etc.

9a. ORIGINATOR'S REPORT NUMBER(S): Enter the official report number by which the document will be identified and controlled by the originating activity. This number must be unique to this report.

9b. OTHER REPORT NUMBER(S): If the report has been assigned any other report numbers (either by the originator or by the sponsor), also enter this number(s).

10. AVAILABILITY/LIMITATION NOTICES: Enter any limitations on further dissemination of the report, other than those imposed by security classification, using standard statements such as:

(1) "Qualified requesters may obtain copies of this report from DDC."

(2) "Foreign announcement and dissemination of this report by DDC is not authorized."

(3) "U. S. Government agencies may obtain copies of this report directly from DDC. Other qualified DDC users shall request through

_____ ."

(4) "U. S. military agencies may obtain copies of this report directly from DDC. Other qualified users shall request through

_____ ."

(5) "All distribution of this report is controlled. Qualified DDC users shall request through

_____ ."

If the report has been furnished to the Office of Technical Services, Department of Commerce, for sale to the public, indicate this fact and enter the price, if known.

11. SUPPLEMENTARY NOTES: Use for additional explanatory notes.

12. SPONSORING MILITARY ACTIVITY: Enter the name of the departmental project office or laboratory sponsoring (*paying for*) the research and development. Include address.

13. ABSTRACT: Enter an abstract giving a brief and factual summary of the document indicative of the report, even though it may also appear elsewhere in the body of the technical report. If additional space is required, a continuation sheet shall be attached.

It is highly desirable that the abstract of classified reports be unclassified. Each paragraph of the abstract shall end with an indication of the military security classification of the information in the paragraph, represented as (TS), (S), (C), or (U).

There is no limitation on the length of the abstract. However, the suggested length is from 150 to 225 words.

14. KEY WORDS: Key words are technically meaningful terms or short phrases that characterize a report and may be used as index entries for cataloging the report. Key words must be selected so that no security classification is required. Identifiers, such as equipment model designation, trade name, military project code name, geographic location, may be used as key words but will be followed by an indication of technical context. The assignment of links, rules, and weights is optional.

1.B

RESEARCH ON RARE EARTH-COBALT ALLOYS
AND COMPOUNDS

Jacques Schweizer

University of Dayton Research Institute

FOREWORD

The following report was prepared by Dr. Jacques Schweizer, covering the work he accomplished in the year he spent in the United States as a Visiting Scientist. The report consists of a collection of papers, articles, and presentations which Dr. Schweizer initiated and participated in as principal investigator.

This technical report has been reviewed and is approved for publication.

CHARLES E. EHRENFRIED
MAJOR, USAF
Chief, Electromagnetic Materials Br.
Materials Physics Division
Air Force Materials Laboratory

ii

ABSTRACT

This report contains a collection of six papers dealing with some magnetic properties of rare earth-cobalt alloys and the crystalline and magnetic structures of some rare earth-cobalt intermetallic phases.

The variation of coercivity as a function of the temperature of annealing or sintering is reported for compacts of a single-phase $PrCo_5$ powder and also for a mixture of $PrCo_5$ with an additive richer in praseodymium.

A previously unidentified thermal event observed in some praseodymium-cobalt alloys is shown to be the peritectic reaction temperature of a new phase, Pr_5Co_{19}. The structures of the two crystallographic modifications of Pr_5Co_{19} are given.

The crystal structures of two previously unreported phases, $Pr_2Co_{1.7}$ and $Nd_2Co_{1.7}$ are given. It is shown that the phase designated as La_xCo in earlier work is actually $La_2Co_{1.7}$ and isostructural to the praseodymium and neodymium phases.

The magnetic structures of the compound $Pr_2Co_{1.7}$ and $Nd_2Co_{1.7}$ have been determined by neutron diffraction experiments conducted at room temperature and helium temperatures. Results of these experiments are presented.

A relatively simple technique for determining the easy axis of magnetization in a material with a large magnetocrystalline anisotropy by means of x-ray diffraction is described. The easy magnetic axes of most of the known R_2Co_{17} and R_2Fe_{17} phases, utilizing this technique, are reported.

The crystal structure of $Ho_{12}Co_7$ is reported. It is shown that this phase corresponds to the phase labeled Ho_xCo in the Ho-Co phase diagram.

TABLE OF CONTENTS

Preceding page blank

LIST OF ILLUSTRATIONS

LIST OF TABLES

INTRODUCTION

This report summarizes the work I have done at the Research Institute of the University of Dayton during my one-year stay from October 1970 to October 1971. At first I performed a literature survey of the R_2Fe_{17} compounds, which had been requested. The results of this were reported in AFML-TR-71-36. Subsequently, I was rather free to investigate any aspect of the crystal structures or magnetic properties of the rare earth-cobalt compounds with a view toward a better understanding of the outstanding properties of some of these as permanent magnets.

First I was involved with Dr. Karl J. Strnat and Dr. James B. Y. Tsui, of the University of Dayton Electrical Engineering Department, in the sintering of $PrCo_5$ magnets with Pr-Co additive. Dr. Tsui had just obtained very exciting results on the sintering-temperature dependence of the magnet properties. I contributed to the discussions that led to the postulation of a shell model for the pinning sites. This work is reported in Chapter I and a paper on it was presented at the International Conference on Magnetics at Denver in April 1971.

In the meantime I tried to obtain further details by means of x-ray diffraction on the sintered magnets. Most of the patterns taken on magnets of good properties exhibited extra unknown lines, and this finding induced me to undertake a complete study of the alloys whose composition lies between Pr_2Co_7 and $PrCo_5$. On a number of samples, prepared by Mr. Robert E. Leasure, University of Dayton Research Institute (UDRI),

in the arc furnace, I ran x-ray diffraction experiments while at the same time Mr. Adolf Biermann (UDRI) performed differential thermal analysis experiments. The constant interaction with him and frequent comparison of his results and mine was very fruitful. It allowed me to show the existence and to find the crystal structure of two new compounds of the composition Pr_5Co_{19}. These structures are reported in Chapter II. But the existence of these new phases does not solve the problem of the extra lines found on the sintered-magnet diffraction diagrams. Investigation of this problem must be continued.

Because the phase nature of the Pr-Co additive was unknown, Dr. Tsui and I undertook the study of the phases present in this alloy. It turned out that this alloy was almost single phase, but this phase was not one of the known ones. We first determined its exact composition, helped by metallographic pictures which were made by Mr. Andrew Kraus of UDRI, then selected single crystals and studied these crystals with the Weissenberg camera. Again the samples used were prepared by Robert Leasure in the arc furnace. We solved the structure of this compound which has the composition $Pr_2Co_{1.7}$, and the results of this effort are reported in Chapter III. A paper on this work was presented at the 9th Rare Earth Conference at Blacksburg, Virginia, in October 1971. Some of the very unusual crystallographic aspects of this structure were also reported at the American Crystallographic Association Meeting at Ames, Iowa, in August 1971. I must point out that I had very fruitful discussions with

Dr. Karel Toman, Professor of Crystallography at Wright State University about the unusual properties of that compound.

I then carried out neutron diffraction experiments on this compound and on the related compound $Nd_2Co_{1.7}$, at Oak Ridge National Laboratory (ORNL), to determine their magnetic structure. These experiments are explained in Chapter IV. I want to emphasize the fact that all the neutron facilities were generously put at my disposal during two weeks by the Neutron Diffraction Group and that Dr. Ray Child (ORNL) very kindly assisted me in the experimentation.

In another effort, also in collaboration with Dr. Tsui, I applied an x-ray method formerly used at Grenoble to determine the easy axis of magnetization of the R_2Co_{17} and R_2Fe_{17} compounds. The method and results are presented in Chapter V. This technique was subsequently used by Mr. Charles Shanley, a graduate student in Materials Science at the University of Dayton, to study the $R_2(Co_xFe_{1-x})_{17}$ compounds and has allowed him to find very interesting results.

Finally, in collaboration with Lt. Wade Adams of the Electromagnetic Materials Branch, Physics Division, Air Force Materials Laboratory, I studied the crystal structure of the compound reported as Ho_xCo in the literature and which appeared to be $Ho_{12}Co_7$. The results of this structure study are reported in Chapter VI. In the course of this investigation, I was very efficiently helped by Miss Kathy King, a high school student who was assigned as an apprentice to the University of Dayton Magnetics Laboratory for the summer. The computer calculations were carried out

partly at the Wright Patterson Computer Center by Wade Adams and partly

at the University of Dayton Computer Center with the programs and the

help of Dr. Albert Fratini, Professor in the Chemistry Department.

CHAPTER I

COERCIVITY OF HEAT TREATED Pr-Co POWDER COMPACTS

J. Schweizer, K. J. Strnat and J. B. Y. Tsui
University of Dayton, Dayton, Ohio 45409

ABSTRACT

The variation of coercivity as a function of the temperature of annealing or sintering is reported for compacts of a single-phase $PrCo_5$ powder and also for a mixture of $PrCo_5$ with an additive richer in praseodymium. For single-phase $PrCo_5$, the intrinsic coercive force decreases steadily with increasing heat-treating temperature and shows a minor peak near $1000^\circ C$. For magnets made with the additive, the curve of $_MH_c$ vs. T has two peaks, one at about $1050^\circ C$ and another at $1120^\circ C$. This behavior can be correlated with thermal events in the Pr-Co phase diagram. It is interpreted in terms of a model which assumes that pinning sites for domain walls exist which are concentrated in shells forming on the surface of $PrCo_5$ grains during the sintering. These shells are thought to consist of Pr-Co compounds having lower melting points than $PrCo_5$ and to be epitaxial layers on or between the $PrCo_5$ grains into which walls can travel from the latter.

INTRODUCTION

It was previously reported[1] that upon heating of $SmCo_5$ powder compacts their coercivity first decreases with increasing temperature but then goes through a pronounced and very high maximum near $1050^{\circ}C$. We conducted similar experiments with $PrCo_5$, hoping that an analogous effect could be found for this alloy. Its existence would be of vital importance for the successful production of magnets from $PrCo_5$, since the intrinsic coercive force of $PrCo_5$ powders prepared by grinding is only marginal[2]. The effect is also of great significance for the sintering of magnets since the coercive force maximum for $PrCo_5$ occurs in the temperature range where the compacts bond and densify well.

EXPERIMENTS AND RESULTS

Following Westendorp,[1] we first heat treated single-phase powders of $PrCo_5$. This $PrCo_5$ was prepared by arc melting and homogenized by annealing at $1050^{\circ}C$. The buttons were then crushed and powdered by hand grinding in a mortar. The powders were heat treated in evacuated quartz tubes at temperatures up to $1100^{\circ}C$ for 30 minutes. After cooling, the powders were mixed with epoxy cement and bonded while aligned in a magnetic field. Magnetization curves were measured on these samples. The coercive force dropped steadily with increasing temperature, then rose only slightly to a minor peak of 800 Oe near $1000^{\circ}C$.

It is well known now[3] that there is another possibility for increasing the coercive force of RCo_5 powder compacts, namely, liquid phase sintering, which is in fact evolving as an important method of magnet production. In

this technique one mixes and presses RCo_5 powder with an additive powder of an alloy richer in rare earth which becomes liquid at the sintering temperature. Magnets prepared properly that way have high density, high coercive force and a high energy product.

We performed heat-treating experiments on $PrCo_5$ powder blended with powder of an alloy of 69 wt.% Pr and 29 wt.% Co ad the rare earth-rich additive and studied the influence of temperature on coercive force and energy product of the magnets. Details of the procedure used and the results of experiments to determine the optimum values of other parameters are presented in another paper.[4] The conditions used here were: 6 minutes grinding time in an attritor-type ball mill for the $PrCo_5$ and a proportion of 80 wt.% $PrCo_5$ to 20 wt.% Pr-Co additive. The nominal overall composition of the powder mixture was between the compositions of Pr_2Co_7 and $PrCo_5$. When the same sample was reused for experiments at different and increasing temperatures, the behavior of the coercive force as a function of temperature was roughly the same as for pure $PrCo_5$, but the peak at 1000°C became more pronounced, $_MH_c$ rising from 1000 Oe at 800°C to 1800 Oe at 1000°C and dropping to 250 Oe at 1120°C as can be seen in Figure 1 (dashed curve).

In the next experiment we prepared a new sample for each sintering temperature. A number of compacts were pressed from the same mixture of powders and annealed for 30 minutes at different temperatures. The variation of the coercive force is also shown in Figure 1 (solid line). The

formerly observed peak is now more pronounced and it is followed by a sharp second minimum at $1100^{\circ}C$ and by an equally sharp maximum of 6700 Oe at $1120^{\circ}C$.

Finally, a last experiment showed that a heat treatment of 30 minutes at $1120^{\circ}C$ brings the coercive force of a sample previously sintered at $1100^{\circ}C$ up from 1200 Oe to 5700 Oe, and that a second heat treatment of 30 minutes at 1100° on the same sample brings it down again.

Physical density values of 7.5 to 8.0 g/cm^3 are reached for sintering temperatures above $1100^{\circ}C$. Maximum energy products were computed and are reported in Figure 2, together with a replot of $_MH_c$. Magnets sintered between $1120^{\circ}C$ and $1160^{\circ}C$ have $(BH)_{max}$ values higher than 15 MGOe.

DISCUSSION

The coercivity of RCo_5 particles, and more particularly of $SmCo_5$, have been discussed either in terms of domain nucleation or in terms of pinning of Bloch walls. In particular, Zijlstra[5] proposed a model in which the pinning sites are concentrated in a magnetically hard shell close to the surface of each particle. The analysis of the temperature dependence of the coercive force of the sintered $PrCo_5$ magnets and a comparison with the Pr-Co phase diagram[6] has lead us to adopt principally his model. In the following we shall discuss our observations qualitatively in these terms, extending Zijlstra's model and trying to develop some concepts about the possible physical nature of the shell. Actually, the two peaks seen in the variation of $_MH_c$ (Figures 1 and 2) are located at temperatures rather clearly identifiable in the phase diagram: the first at the peritectic

temperature of the intermetallic compound $PrCo_3$ ($1063^\circ C$) and the second

between the peritectic temperature of the compound Pr_2Co_7 ($1128^\circ C$) and the

transformation temperature of Pr_2Co_7 from the hexagonal to the rhombohedral

crystal structure ($1119^\circ C$), these two temperatures being very close to one

another. During a sintering experiment the system tends to approach

thermodynamic equilibrium rather rapidly when the temperature is that high.

At the surface of the $PrCo_5$ grains, which are stable at the sintering

temperatures (the peritectic temperature of $PrCo_5$ is $1232^\circ C$), an epitaxial

shell of Pr_2Co_7 may grow below 1128°, or even one of $PrCo_3$ below $1063^\circ C$.

These layers may contain a number of pinning sites either because of the

existence of stacking faults or the presence of oxide particles.

It is known that the crystal structure of the compounds Pr_2Co_7, both

in its rhombohedral high and its hexagonal low temperature form, and that

of $PrCo_3$ are very similar to each other and to the structure of $PrCo_5$.

They differ merely by some atomic substitutions and by the way the different

planes of atoms are stacked. Consequently, epitaxy among these different

compounds is very common and is generally accompanied by numerous

stacking faults.[7] All these compounds are also ferromagnetic at room

temperature and have a strong uniaxial anisotropy. Stacking faults in them

may be active as pinning sites. If the sintering temperature is below $1062^\circ C$,

an epitaxial layer of $PrCo_3$ may occur but it would disappear on heating

above the peritectic temperature of that compound. In the same way, a

layer of epitaxial Pr_2Co_7 may grow below $1128^\circ C$ and will redissolve into

the liquid phase upon heating above this temperature. During rapid cooling

from such a high sintering temperature, only a very thin layer of epitaxial Pr_2Co_7 can grow that is likely to be rather imperfect because of the high rate of formation. On the other hand, any thicker and more perfect layer of Pr_2Co_7 grown during annealing between $1119^{\circ}C$ and $1128^{\circ}C$ has to change from the rhombohedral to the hexagonal form during the cooling, and this transformation would cause a large number of stacking faults. So the number of stacking faults has to be a maximum for a sintering temperature of around $1128^{\circ}C$. Similar arguments apply when the annealing is done around $1062^{\circ}C$, with an epitaxial $PrCo_3$ layer (over an intervening thin layer of Pr_2Co_7) playing the role which the Pr_2Co_7 plays at the upper $_MH_c$ peak.

Another possibility for creating pinning sites is the precipitation of small oxide particles. It was stated[8] that an important function of the additive during the sintering process is to remove oxygen from the surface of the $PrCo_5$ grains. During the rapid heating of the powder compacts, the original $PrCo_5$ grains are surrounded by liquid alloy and this Pr-rich liquid phase will react with most of the adsorbed oxygen present on the surface of the $PrCo_5$ particles before the latter has a chance to diffuse into the $PrCo_5$. We presume that this oxygen is in solution in the liquid phase, but that the solubility of oxygen in the solid is rather small.

As a consequence, precipitation of small rare-earth oxide particles will take place in the rare earth-rich regions between the $PrCo_5$ grains when the material there solidifies. When the solidification occurs rapidly, as it did in our experiments, the oxide particles may be so small as to be very efficient pinning sites for domain walls. The precipitate effective for

the magnetic hardening of the magnets by this mechanism would be that

present in the thin epitaxial layer of Pr_2Co_7 formed around the $PrCo_5$ grains.

During additional sintering or annealing in the completely solid state below

the peritectic temperature, these oxide precipitates may grow beyond a

size where they are effective pinning sites so that the coercive force

would decline. If for some reason the original oxide particle size was

below the optimum for pinning, this process could be preceded by an

increase of H_c on further annealing.

We have proposed two possibilities for explaining the nature of the

pinning sites. Both processes may act together, or one may be dominant,

or still another mechanism may exist. But the correspondence between

the sintering temperatures at which the peaks in coercivity occur and the

temperatures of the different events shown by the phase diagram suggests

strongly that such a model has indeed some validity. The distinguishing

feature of the model is the presence of an epitaxial shell of a lower-melting

magnetic R-Co compound which surrounds the $PrCo_5$ grains, has a high

concentration of pinning sites and is thus capable of trapping domain walls

which travel into it from the $PrCo_5$ grains. The $PrCo_5$ grains themselves

are thought to be become rather perfect crystals during the heat-treating

process, so they have a low wall-motion coercivity and a very high critical

field for internal domain nucleation.

Similar experiments were also carried out with a Sm-Co additive

instead of Pr-Co. The results are qualitatively the same, the two peaks

occurring at a slightly higher temperature. This is probably due to the

higher melting points of the corresponding samarium compounds. The model is assumed to be equally applicable in this case -- as indeed it may be to all R-Co alloy powder combinations liquid-phase sintered under similar circumstances.

REFERENCES

1. F. F. Westendorp, <u>Solid State Commun.</u>, 8:139, (1970).

2. K. Strnat and J. Tsui, <u>Proceedings of the Eighth Rare Earth Research Conference, Reno, Nevada</u>, Vol. I, p. 3, 1970.

3. M. G. Benz and D. L. Martin, <u>Appl. Phys. Lett.</u>, 17:176, (1970).

4. J. Tsui and K. Strnat, <u>IEEE Trans. Magnet.</u>, MAG-7:427, (1970).

5. H. Zijlstra, <u>J. Appl. Phys.</u>, 41:4881, (1970).

6. A. E. Ray and G. I. Hoffer, <u>Proceedings of the Eighth Rare Earth Research Conference, Reno, Nevada</u>, Vol. II, p. 524, 1970.

7. E. F. Bertaut, R. Lemaire, and J. Schweizer, <u>Bull. Soc. Franc. Miner. Crist.</u>, 88:580, (1965).

8. R. E. Cech, <u>J. Appl. Phys.</u>, 41:5247, (1970).
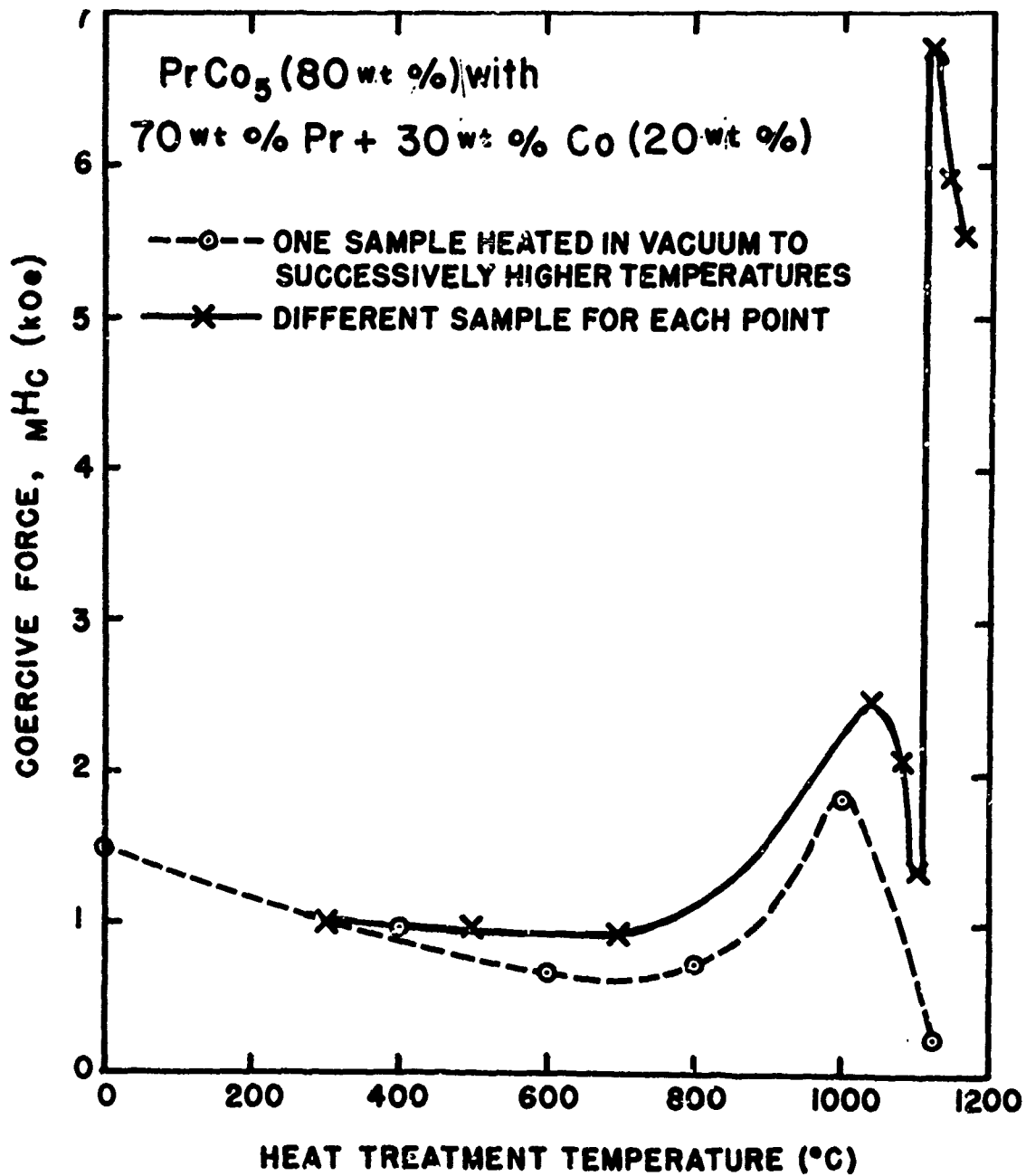
Figure 1. Variation of the intrinsic coercive force with the temperature of the heat treatment for $PrCo_5$ powder compacts.
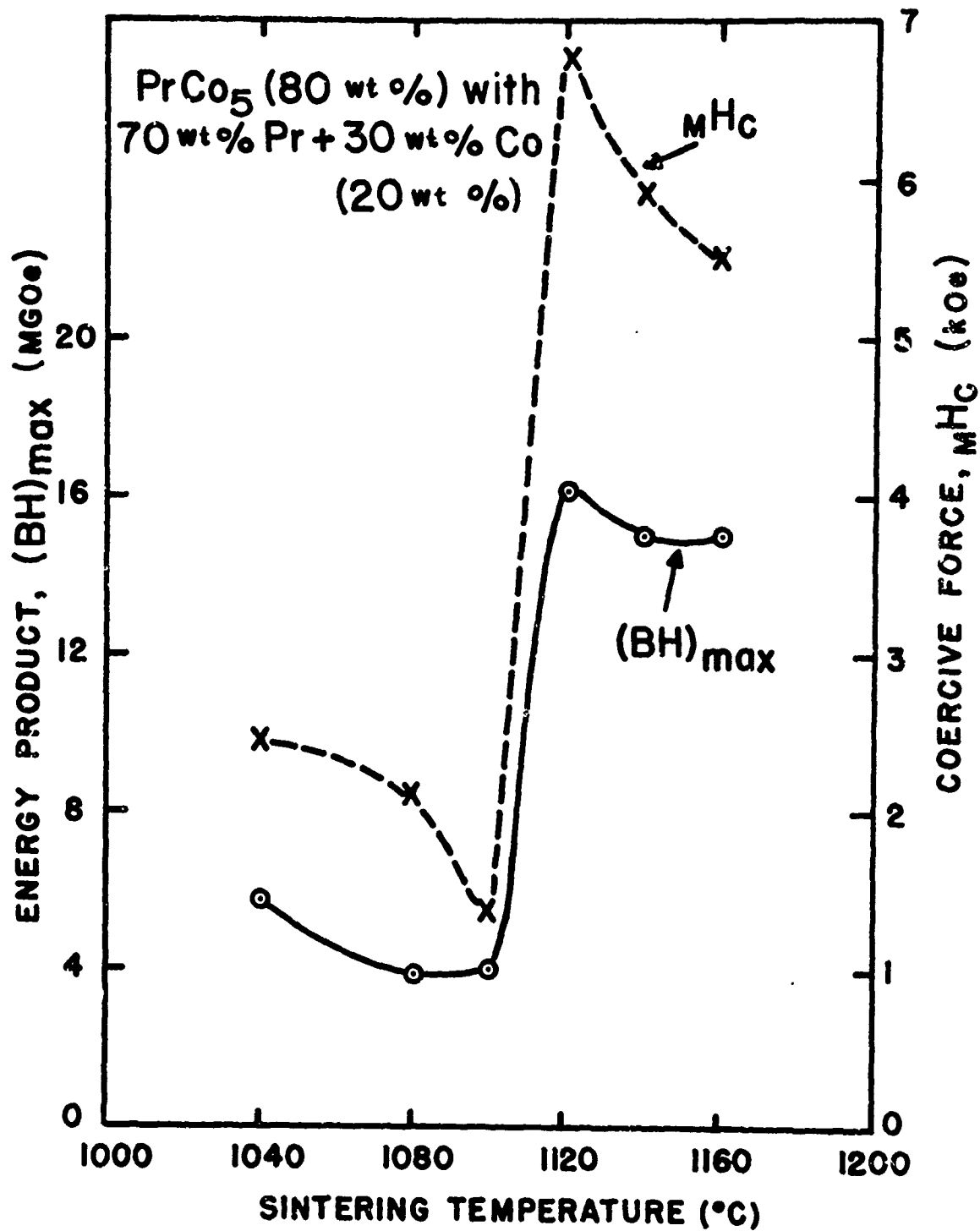
Figure 2. Coercivity and energy product for liquid-phase sintered PrCo$_5$ magnets.

CHAPTER II

EXISTENCE AND CRYSTAL STRUCTURE OF THE TWO NEW PHASES,
Pr_5Co_{19}
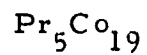
It was known[1] that between the compounds $PrCo_5$ and $PrCo_2$ two other compounds existed: Pr_2Co_7 and $PrCo_3$. In the interpretation of Differential Thermal Analysis (DTA) experiments, two thermal arrests were associated with the Pr_2Co_7 phase (Figure 1): the higher one was attributed to the peritectic reaction and the lower one to a solid state transformation in Pr_2Co_7. Actually two crystal structures exist for Pr_2Co_7[2]: one is hexagonal (a = 5.060 Å, c = 24.42 Å) and the other rhombohedral (a = 5.060 Å, c = 36.63 Å). In quenched samples one can only get a mixture of the two phases, and by annealing the hexagonal phase is stabilized.

In order to check the correctness of this explanation of the two thermal events, Mr. Adolf Biermann of UDRI made a DTA experiment on a Sm_2Co_7 alloy which also exhibits the two crystal structures, the rhombohedral and the hexagonal[2]. No thermal event corresponding to a solid state transformation was found (Figure 2). This led to the conclusion that the hexagonal-rhombohedral transformation has indeed too low a latent heat to be seen in our DTA experiments, and that therefore the explanation for the two thermal events in Pr_2Co_7 must be found elsewhere.

To pursue this question further, I requested a number of alloys of compositions between Pr_2Co_7 and $PrCo_5$ and analyzed them by x-ray diffraction. The as-cast samples revealed a mixture of $PrCo_5$ and Pr_2Co_7

(mostly hexagonal, but there was also some of the rhomgohedral form present). On the x-ray powder patterns of the samples annealed between $1050^{\circ}C$ and $1075^{\circ}C$ new lines appeared that belonged neither to Pr_2Co_7 nor to $PrCo_5$. This was evidence of the existence of a new phase. The composition of this new phase seemed to be close to 21 at.% Pr, the composition for which the x-ray patterns showed a minimum of Pr_2Co_7 and $PrCo_5$ impurity lines.

At that point of the study, a single crystal analysis of the new phase would have been needed, but several attempts to isolate a single crystal were unsuccessful. The only x-ray analysis available was on powders, and as the cell of that new phase was expected to be fairly large, the only possibility was to make some theoretical assumptions about the crystal structure of the new compound and check them against the powder x-ray diffraction results. So I assumed that the composition might be Pr_5Co_{19} and imagined what could be the possible crystal structure for such a compound. The reason for this choice is that it has been shown[3] that the compounds RCo_2, RCo_3 and R_2Co_7 can be deduced from RCo_5 by ordered substitutions of atoms; one rare earth atom is substituted for a cobalt atom in every n cells of RCo_5

$$n = 1 \qquad RCo_5 + R - Co \rightarrow 2RCo_2$$

$$n = 2 \qquad 2RCo_5 + R - Co \rightarrow 3RCo_3$$

$$n = 3 \qquad 3RCo_5 + R - Co \rightarrow 2R_2Co_7$$
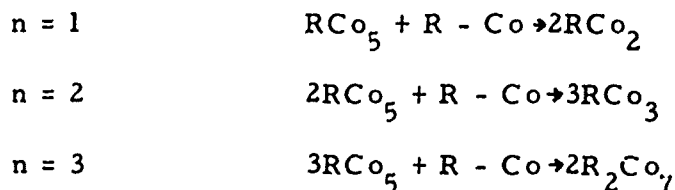
In each case the stacking of the n cells of RCo_5 may be either of the type ABAB.., which gives an hexagonal structure ($P6_3/mmc$), or of the

type ABCABC..., which leads to a rhombohedral structure ($R\overline{3}m$). So, when looking for a new compound it is tempting to go one step further and to write:

$$n = 4 \qquad 4PrCo_5 + Pr - Co \rightarrow Pr_5Co_{19}$$
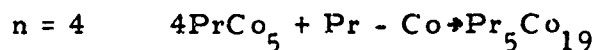
with two possible crystal structures: hexagonal and rhombohedral. These modifications are represented in Figure 3, with atom positions given in Tables I and II. These compounds would have a composition of 20.8 at.% Pr, in fairly good agreement with the observations, and the following lattice constants:

$$a \approx a \text{ of } PrCo_5$$

$$c_{hex} \approx 8. \, c \text{ of } PrCo_5$$

$$c_{rhomb} \approx 12. \, c \text{ of } PrCo_5$$

I ran a calculation to determine the diffraction angles of the x-rays diffracted by these two crystal structures and the expected intensities of the reflections. Compairson with the observed reflections (Table III) showed that both compounds exist and are present in the observed samples. The rhombohedral compound predominates in all the samples studied, but the presence of the hexagonal compound is shown by the existence of the strongest of its superstructure reflections, (1 0 9). This line is quite sharp in a sample of 21.1 at.% Pr annealed at $1050^{\circ}C$ but strongly broadened in the three other samples: 21.2 at.% Pr annealed at $1075^{\circ}C$, 20.8 at.% Pr annealed at $1050^{\circ}C$, and 20.5 at.% Pr annealed at $1050^{\circ}C$. The rhombohedral lines are sharp in all four samples. This may be interpreted either in terms of a small coherence dimension for the

hexagonal compound or as the presence of many stacking faults occurring in this crystal structure. No refinement of the structures has been carried out; this explains the rather poor agreement between calculated and observed intensities for the large indices.

The measured lattice constants of the two compounds are:

$$a_{hex} = 5.053 \text{ Å} \qquad c_{hex} = 32.47 \text{ Å}$$

$$a_{rhomb} = 5.053 \text{ Å} \qquad c_{rhomb} = 48.71 \text{ Å}$$

These lattice parameters fit nicely with those of $PrCo_3$, Pr_2Co_7 and $PrCo_5$ when plotted versus composition (Figure 4).

We are now able to understand the two events observed on the DTA experiments: The lower one corresponds to the peritectic transformation of Pr_2Co_7; the upper is at the peritectic temperature of Pr_5Co_{19}. None of the solid state transformations in Pr_2Co_7 or in Pr_5Co_{19} were observed by DTA.

The shell model explanation of the origin of the intrinsic magnetic coercive force given in Chapter I is still applicable with this new interpretation of the DTA events. I would even suggest that the peak in coercivity at $1120°C$ observed in sintered $SmCo_5$ magnets by Das[4], that does not correspond to a peritectic transformation in the way we proposed in the shell-model interpretation for $PrCo_5$ magnets, corresponds to the rhombohedral-to-hexagonal transformation of Sm_2Co_7. This point cannot be checked by DTA but only by high temperature x-ray diffraction. Such a verification would be very interesting for the understanding of magnet sintering.

REFERENCES

1. A. E. Ray and G. I. Hoffer, <u>Proceedings of the Eighth Rare Earth Research Conference, Reno, Nevada</u>, Vol. I, p. 524, 1970.

2. J. Schweizer, Ph. D. Thesis, University of Grenoble, p. 39 1968.

3. E. F. Bertaut, R. Lemaire, and J. Schweizer. <u>Bull. Soc. Franc. Miner. Crist.</u>, 88:580, 1965.

4. D. Das, <u>IEEE Trans. Magnet.</u>, MAG-7:432 (1971).

Figure 1. Differential thermal analysis of Pr_2Co_7, alloy AR-403, 22.2 at.% Pr – 77.8 at.% Co, homogenized at $1100°C$ for 6 hours.
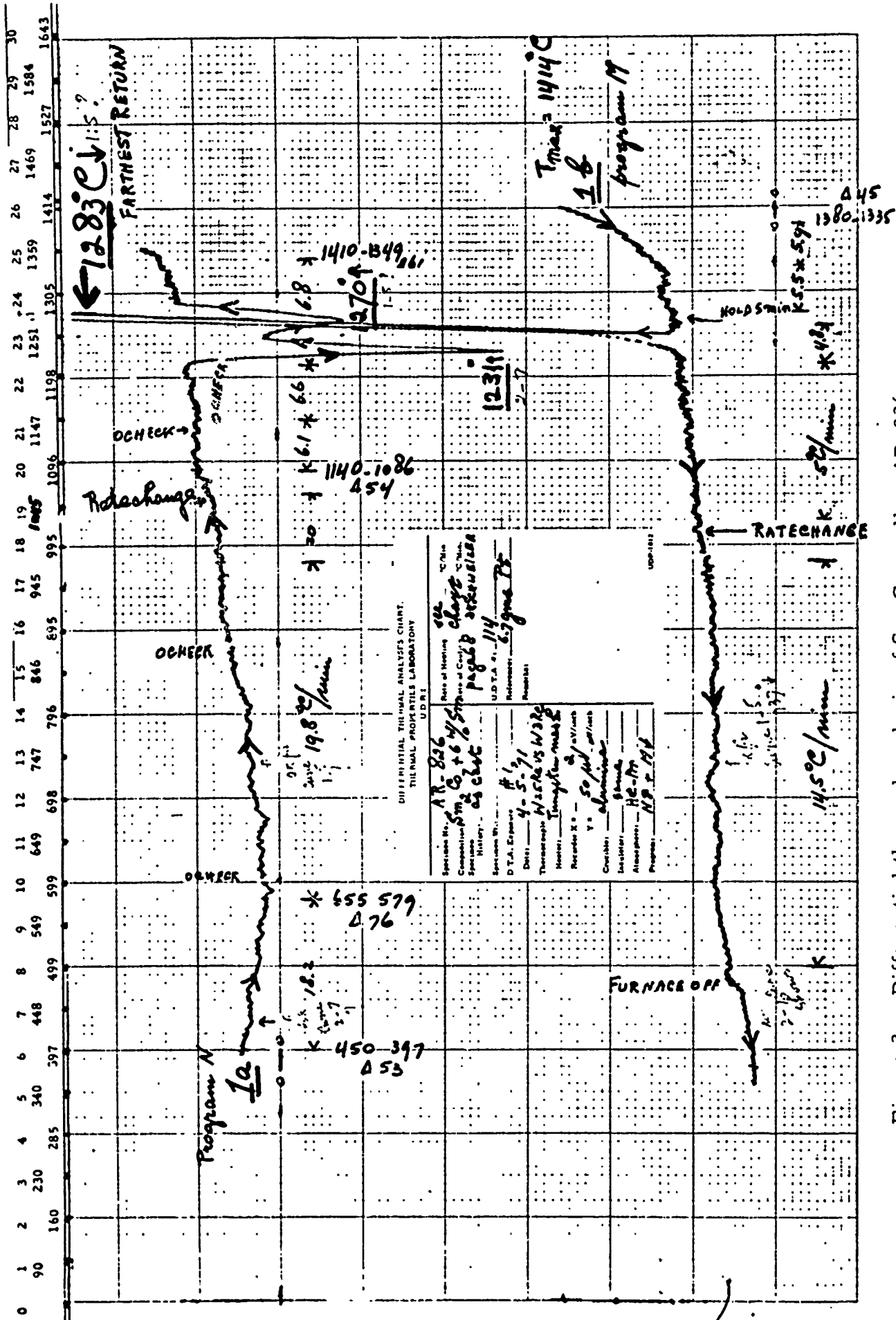
Figure 2. Differential thermal analysis of Sm_2Co_7, alloy AR-826, as cast.
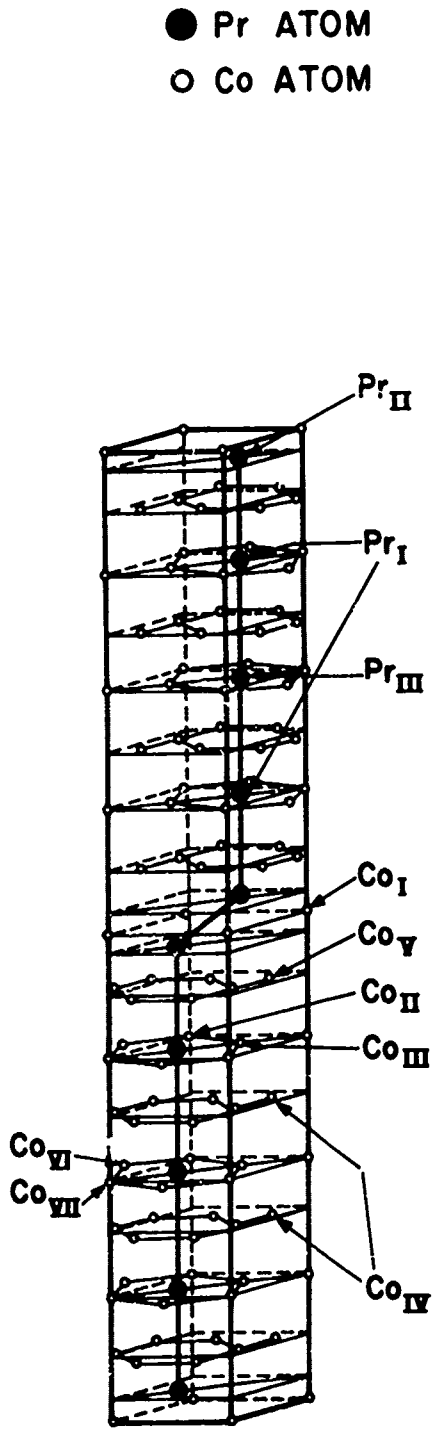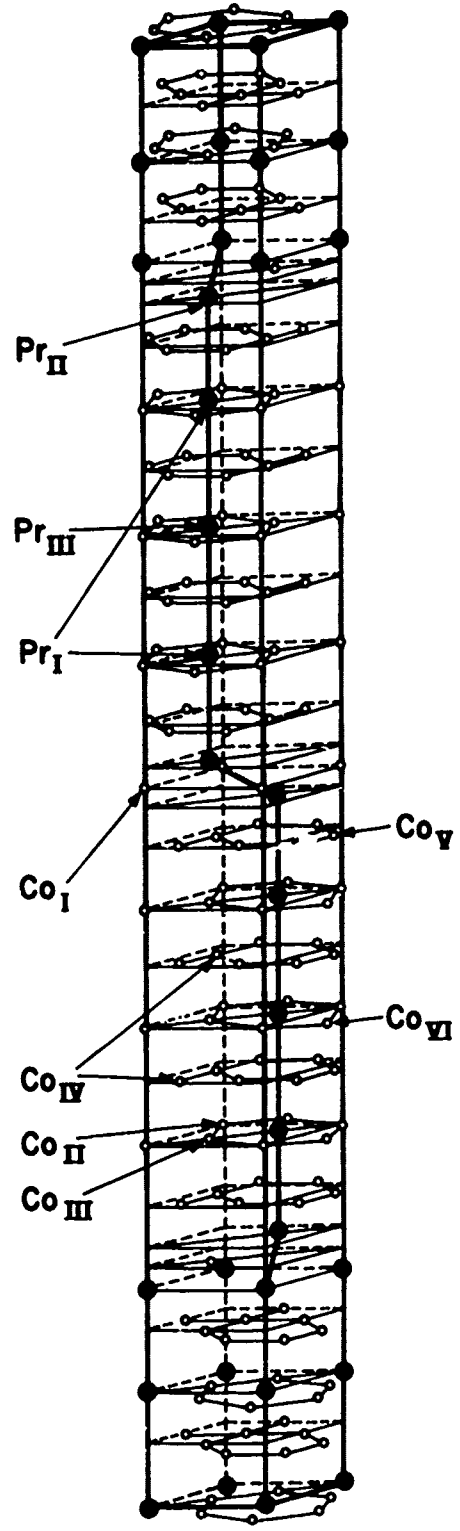
Figure 3. Crystal Structures of the hexagonal and rhombohedral forms of Pr_5Co_{19}.
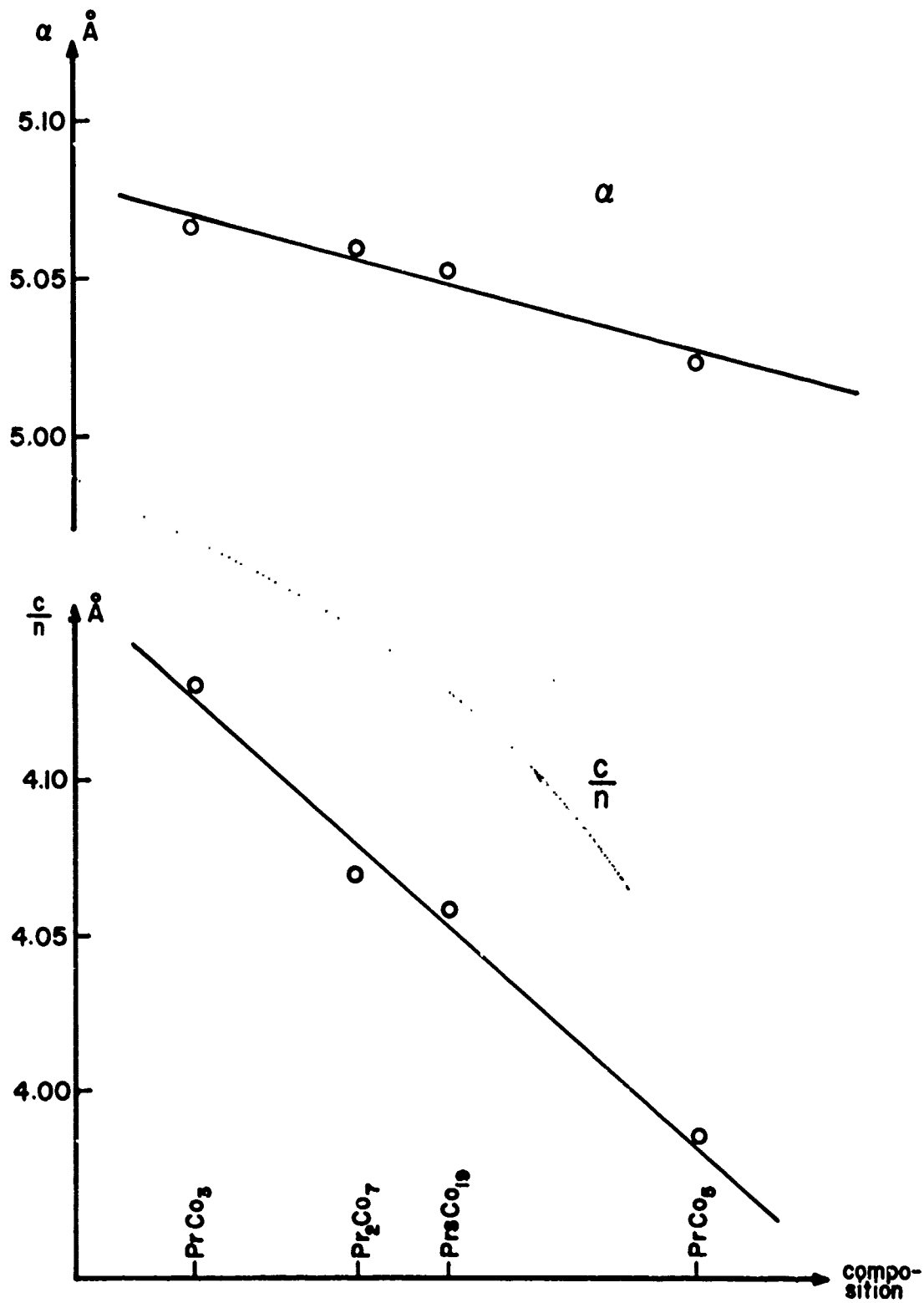
Pr_5Co_{19}

Figure 4. Lattice constants versus composition for the hexagonal or rhombohedral phases of $PrCo_3$, Pr_2Co_7, Pr_5Co_{19}, and $PrCo_5$.

TABLE I

HEXAGONAL Pr$_5$Co$_{19}$

Space Group P6$_3$/mmc

a = 5.053 Å,   c = 32.47 Å

Atom	Position	x	y	z
Pr$_I$	4f			0.125
Pr$_{II}$	4f			0.021
Pr$_{III}$	2c			
Co$_I$	2a .			
Co$_{II}$	4e			0.125
Co$_{III}$	4f			0.875
Co$_{IV}$	12k	0.833		0.187
Co$_V$	12k	0.833		0.064
Co$_{VI}$	2d			
Co$_{VII}$	2b			

2a: (0, 0, 0); (0, 0, 1/2).

2b: (0, 0, 1/4); (0, 0, 3/4).

2c: (1/3, 2/3, 1/4); (2/3, 1/3, 3/4).

2d: (1/2, 2/3, 3/4); (2/3, 1/3, 1/4).

4f: (1/3, 2/3, z); (2/3, 1/3, $\bar{z}$); (2/3, 1/3, 1/2 +z); (1/3, 2/3, 1/2-z).

12k: ± (x, 2x, z); (2$\bar{x}$, $\bar{x}$, z); (x, $\bar{x}$, z); (x, 2x, 1/2-z); (2$\bar{x}$, $\bar{x}$, 1/2-z); (x, $\bar{x}$, 1/2-z).

TABLE II

RHOMBOHEDRAL Pr_5Co_{19}

Space Group $R\bar{3}m$

Hexagonal Indexation: $a = 5.053\overset{\circ}{A}$, $c = 48.71\overset{\circ}{A}$

Atom	Position	x	y	z
Pr_I	6c			0.082
Pr_{II}	6c			0.153
Pr_{III}	3a			
Co_I	3b			
Co_{II}	6c			0.251
Co_{III}	6c			0.415
Co_{IV}	18h	0.500		0.041
Co_V	18h	0.500		0.124
Co_{VI}	6c			0.333

$(0,0,0); (1/3,2/3,2/3); (2/3,1/3,1/3) +$

3a: $(0,0,0)$.

3b: $(0,0,1/2)$.

6c: $\pm (0,0,z)$

18h: $\pm (x,\bar{x},z); (x,2x,z) ; (2\bar{x},\bar{x},z)$.

TABLE III

RHOMBOHEDRAL Pr_5Co_{15}: REFLECTIONS AND INTENSITIES

$$= 2.2909 \text{ Å}$$

h k ℓ	$2\Theta_{cal}$	$2\Theta_{obs}$	pF^2_{cal}	I_{obs}
0 0 3	8.09		0	
0 0 6	16.22		0	
0 0 9	24.44		0	
1 0 1	30.47		2	
-1 0 2	30.84		0	
1 0 4	32.30		2	
0 0 12	32.78		6	
-1 0 5	33.35		0	
1 0 7	36.02		1	
-1 0 8	37.61		0	
1 0 10	41.20		0	
0 0 15	41.31		2	
-1 0 11	43.18		14	
1 0 13	47.46	47.45	117	M[1]
1 0 9(hex)[3]	48.60[3]	48.67[3]		W[3]
-1 0 14	49.74	49.80	71	W
0 0 18	50.08		2	
1 1 0	53.92	54.00	194	S
1 0 16	54.56		14	
1 1 3	54.62		1	
1 1 6	56.69		1	
-1 0 17	57.09		35	
0 0 21	59.18		1	
1 1 9	60.05		1	
1 0 19	62.37		5	

TABLE III (Continued)

h k ℓ	$2\Theta_{cal}$	$2\Theta_{obs}$	pF^2_{cal}	I_{obs}
-2 0 1	63.20	63.35	194	S
2 0 2	63.42		45	
-2 0 4	64.27		23	
1 1 12	64.55	64.70	673	VS
2 0 5	64.90		14	
-1 0 20	65.13		29	
-2 0 7	66.57		18	
2 0 8	67.60		18	
0 0 24	68.72	68.	145	M
-2 0 10	70.04		26	
1 1 15	70.12		17	
1 0 22	70.87		1	
-2 0 11	71.45	71.60	67	W
-1 0 23	73.86		23	
2 0 13	74.63		8	
-2 0 14	76.40		0	
1 1 18	76.67		14	
0 0 27	78.83	79.00	21	VW
1 0 25	80.11		1	
-2 0 16	80.28		0	
1 1 24	92.76	92.80	68	W
2 1 13	98.40	98.80	136	W
-2 1 14	100.14	100.00	84	VW
3 0 0	103.49		116	
		103.45	253	S
-2 0 25	103.85		137	
2 0 26	107.20	107.15	118	VW

TABLE III (Concluded)

h k ℓ	$2\Theta_{cal}$	$2\Theta_{obs}$	pF^2_{cal}	I_{obs}
3 0 12	113.11	113.10	398	S
2 2 0	130.12	130.00	381	S
1 1 36	147.61	147.45	116	S
3 0 24	150.50	150.45	402	M

(1) Intensity:
VS   Very Strong
S   Strong
M   Medium
W   Weak
VW   Very Weak

(2) All the reflections have been listed till $2\theta = 80°$; then only the strongest ones.

(3) Beside the reflection (1 0 9) all the observed lines of Pr_5Co_{19} hexagonal are structure reflections and coincide with those of Pr_5Co_{19} rhombohedral.

CHAPTER III

THE CRYSTAL STRUCTURE OF THE INTERMETALLIC

COMPOUNDS $Pr_2Co_{1.7}$, $Nd_2Co_{1.7}$ and $La_2Co_{1.7}$

J. Schweizer,   K. J. Strnat and   J. B. Y. Tsui
University of Dayton, Dayton, Ohio 45409

ABSTRACT

A crystal structure is reported for the two previously unknown inter-metallic compounds of the approximate compositions $Pr_2Co_{1.7}$ and $Nd_2Co_{1.7}$. The compounds crystallize in a very simple hexagonal cell with parameters a = 4.81 Å, c = 4.09 Å, and a = 4.79 Å, c = 4.07 Å, respectively. This cell contains two rare earth atoms in the positions (2/3, 1/3, 1/4) and 1/3, 2/3, 3/4). These are the positions corresponding to a hexagonal packing ABAB. The cobalt atoms are located in x = y = 0 and form columns parallel to the c-axis along which the Co atoms are in contact with each other. These columns fit into cylindrical interstices between the rare earth atoms. The c-parameter of the cell is too small for two cobalt atoms to be present in both the (0,0,0) and (0,0,1/2) positions, but the shortest distance between rare earth atoms in the basal plane is large enough to permit formation of a continuous row of Co atoms in the z-direction at distances of 2.37 Å, with a stacking period independent of that of the rare earth. The correlation between the Co columns is weak. This gives rise to diffuse planes in reciprocal space perpendicular to the c-axis.

CHAPTER III

THE CRYSTAL STRUCTURE OF THE INTERMETALLIC

COMPOUNDS $Pr_2Co_{1.7}$, $Nd_2Co_{1.7}$ and $La_2Co_{1.7}$

J. Schweizer, K. J. Strnat and J. B. Y. Tsui
University of Dayton, Dayton, Ohio 45409

ABSTRACT

A crystal structure is reported for the two previously unknown inter-metallic compounds of the approximate compositions $Pr_2Co_{1.7}$ and $Nd_2Co_{1.7}$. The compounds crystallize in a very simple hexagonal cell with parameters a = 4.81 Å, c = 4.09 Å, and a = 4.79 Å, c = 4.07 Å, respectively. This cell contains two rare earth atoms in the positions (2/3, 1/3, 1/4) and 1/3, 2/3, 3/4). These are the positions corresponding to a hexagonal packing ABAB. The cobalt atoms are located in x = y = 0 and form columns parallel to the c-axis along which the Co atoms are in contact with each other. These columns fit into cylindrical interstices between the rare earth atoms. The c-parameter of the cell is too small for two cobalt atoms to be present in both the (0,0,0) and (0,0,1/2) positions, but the shortest distance between rare earth atoms in the basal plane is large enough to permit formation of a continuous row of Co atoms in the z-direction at distances of 2.37 Å, with a stacking period indepen-dent of that of the rare earth. The correlation between the Co columns is weak. This gives rise to diffuse planes in reciprocal space perpendicular to the c-axis.

INTRODUCTION

The phase diagrams of cobalt with any of the rare earth metals are characterized by a great number of intermetallic compounds, each of them existing over a very narrow homogeneity range only. This alloying behavior is attributable to the large difference in the atomic radii of the two component metals. An intermediate phase of a given stoichiometric composition usually exists with all or most of the rare earth elements, thus forming a family of isostructural compounds. However, some exceptions from this rule occur, and they are primarily found in the rare earth-rich portions of the phase diagrams and with the light rare earths. As a case in point, the compound R_4Co_3 has been reported to exist with the elements from gadolinium through thulium[1]. This crystal structure does not appear to be stable with the lighter rare earth metals though, and in fact no compound near the equiatomic composition was found in investigations of the cerium-cobalt[2] and the samarium-cobalt[4] phase diagrams. The published diagrams for praseodymium and neodymium with cobalt as the partner[5] show an unexplained thermal arrest in the composition range near 50 at.%.

Studies of the liquid-phase sintering of $PrCo_5$-based permanent magnets using a praseodymium-rich Pr-Co alloy as the sintering additive[6] caused us to investigate more closely the alloys near the equiatomic composition in the Pr-Co system. This work resulted in the identification of a previously unreported compound which also exists with neodymium. The

structure of this compound has been studied and is reported here.

RESULTS AND INTERPRETATION

Alloys samples of various compositions were prepared by both arc and crucible melting of the component metals. The arcmelted buttons were studied in the as-cast condition and after annealing in vacuum at $500^{\circ}C$. The samples containing 74 wt.% showed almost -single-phase structures in either condition. This single-phase composition corresponds to 54 at.% praseodymium and 46 at.%.

X-ray powder patterns were indexed in a hexagonal cell. The lattice constants are a = 4.81 $\overset{o}{A}$ and c = 4.09 $\overset{o}{A}$. At first glance, the very small dimensions of the unit cell seem irreconcilable with the composition, since the number of atoms per cell cannot exceed four and mutual substitutions between praseodymium and cobalt are not expected.

Rotating-crystal diffraction patterns, generated by rotating the sample around the a-axis and the c-axis, showed that the reflections (hkl) were absent when 2h + k = 3 n and l was odd. A very striking feature was noticed in the patterns that were produced by rotating the crystal around the c-axis: Besides the regular layers of reflections corresponding to c = 4.09 $\overset{o}{A}$, weak diffuse layers exist which are also perpendicular to the c-axis and correspond to a distance in the direct lattice of 2.37 $\overset{o}{A}$. Incommensurable with the c value, these diffuse planes are the diffraction pattern of one-dimensional crystals extending parallel to the c-axis. Such an arrangement was first observed by Huml[7]. These linear crystals consist of cobalt atoms which are arranged in regular chains parallel to the c-axis

with $x = y = 0$, and the distance between the nearest neighbors along the chain is 2.37 Å. There is no correlation with respect to z from one chain to the other, and no correlation exists between the z-values of these cobalt atoms and the z-values of the praseodymium atoms which are located in the positions (1/3, 2/3, 2/3; 2/3, 1/3, 1/4) and form the skeleton of the described cell. (See Figure 1.) The observed x-ray intensities fit well with this model as shown in Table I. For the (hk0) reflections, both the praseodymium and the cobalt atoms contribute to the structure factor because it is independent of the z values; for the ($hk\ell$) reflections with $\ell \neq 0$, only the praseodymium atoms contribute to the structure factor because of the lack of correlation between the z coordinates of the cobalt atoms. The composition and cell content deduced from these crystallographic data is $Pr_2Co_{1.7}$. This is in good agreement with the composition for which single-phase microstructures were obtained.

A closer examination of the diffuse layers shows the existence of weak reflections indicating some correlation between the z values of the different rows of cobalt. This is probably due to some small shift of the praseodymium atoms away from their theoretical positions.

The praseodymium positions are the same as those of the atoms in a simple hexagonal compact structure. But because of the presence of the rows of cobalt, the praseodymium stacking in our case is indeed not compact, and the c/a-ratio has the low value of c/a = 0.85. The distance of closest approach between two praseodymium atoms is 3.45 Å, the

distance between a Pr and a Co atom can vary between 2.78 $\overset{o}{A}$ and 3.02 $\overset{o}{A}$.

$Nd_2Co_{1.7}$ has the same crystal structure as $Pr_2Co_{1.7}$, but with the parameters a = 4.79 $\overset{o}{A}$ and c = 4.07 $\overset{o}{A}$.

In the discussion of the hexagonal R_4Co_3 compounds which exist with the heavy rare earths[1], the observed intensities were also explained by assuming that the cobalt atoms located in x = y = 0 were not well correlated in z with the other atoms of the cell. Because of the large number of atoms in that cell, however, the actual observation of diffused planes was impossible there. (The cell dimensions are a$\approx$11.4 $\overset{o}{A}$ and c$\approx$4.0 $\overset{o}{A}$.)

$La_2Co_{1.7}$ exists also and has the same crystal structure as $Pr_2Co_{1.7}$. It corresponds to the compound La_xCo reported by Buschow and Velge[3] and Singh and Raman[8] and misindexed as cubic. Its lattice constants are a = 4.89 and c = 4.31.

REFERENCES

1. R. Lemaire, J. Schweizer, and J. Yakinthos, Acta Cryst.,
    B 25: 710 (1969).

2. F. H. Ellinger, C. C. Land, K. A. Johnson, and V. O. Struebing,
    Trans. Met. Soc. AIME, 236: 1577 (1966).

3. K. H. J. Buschow and W. A. J. J. Velge, J. Less-Common Metals,
    13: 11 (1967).

4. K. H. J. Buschow and A. S. VanDerGoot, J. Less-Common Metals,
    14: 323 (1968).

5. A. E. Ray and G. I. Hoffer, Proceedings of the Eighth Rare Earth
    Research Conference, Reno, Nevada, Vol. II, p. 524, (1970).

6. J. Tsui and K. Strnat, Appl. Phys., 18: 107 (1970).

7. K. Huml, Acta Cryst. 22: 29 (1967).

8. P. O. Singh and A. Raman, Mater. Res. Bull., 3: 843 (1968).
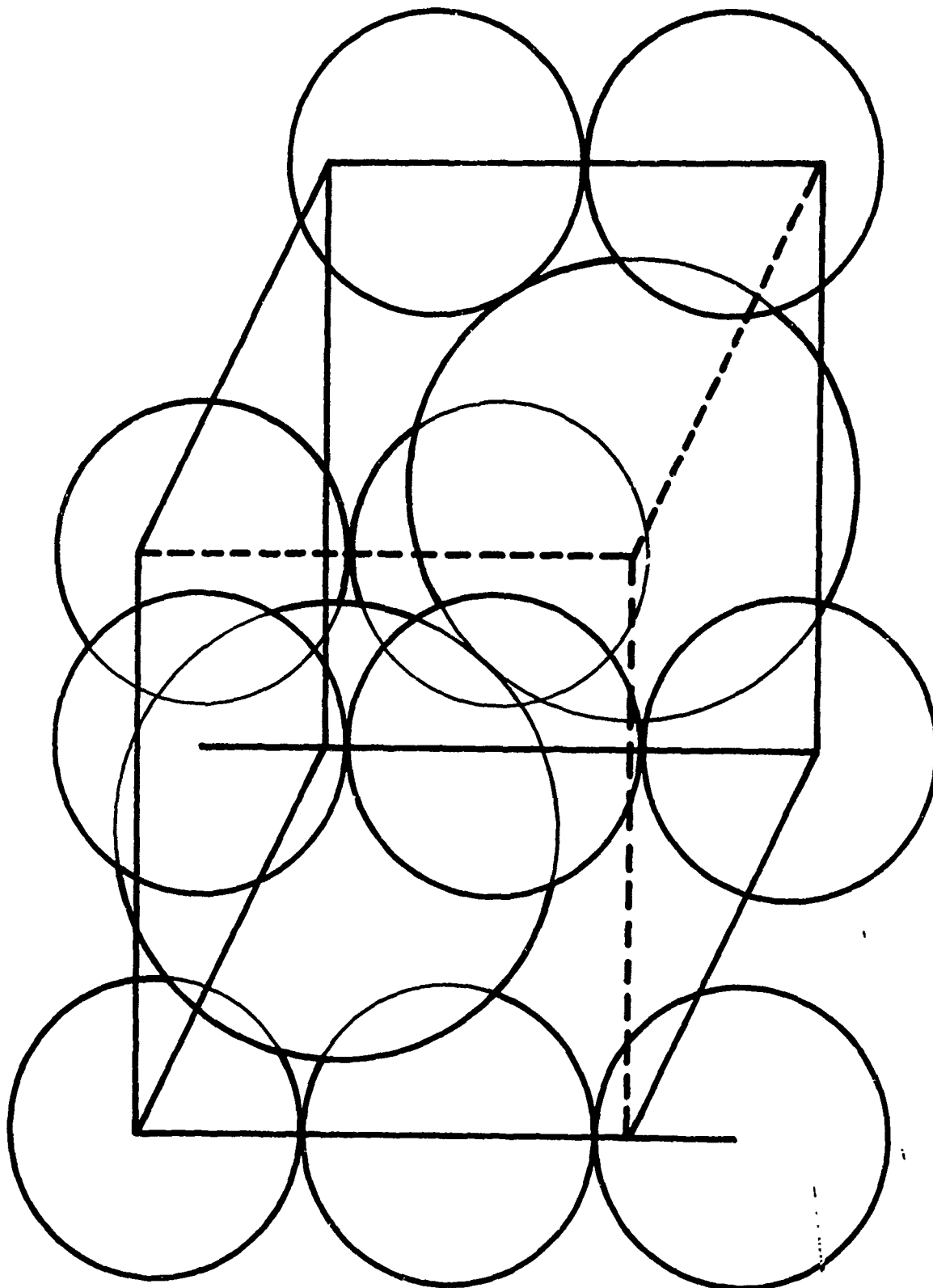
Figure 1. Crystal structure of $Pr_2Co_{1.7}$ and $Nd_2Co_{1.7}$.

TABLE I

$Pr_2Co_{1.7}$: OBSERVED AND CALCULATED INTENSITIES

h k ℓ	$F^2e^{-2w}{}_{obs}$	$F^2e^{-2w}{}_{cal}$	h k ℓ	$F^2e^{-2w}{}_{obs}$	$F^2e^{-2w}{}_{cal}$
1 0 0	90	101	1 0 1	6467	6385
1 1 0	14578	14054	1 1 1	N. O.	0
2 0 0	100	87	2 0 1	4821	4219
2 1 0	89	72	2 1 1	2602	3030
3 0 0	6462	6901	3 0 1	N. O.	0
2 2 0	4308	5213	2 2 1	N. O.	0
4 1 0	2742	2505	3 1 1	1525	1758
3 3 0	1368	1383	4 0 1	1404	1391
6 0 0	738	881	3 2 1	1057	1092
5 2 0	753	682	4 1 1	N. O.	0
4 4 0	320	416			

N. O. = Not Observed

CHAPTER IV

MAGNETIC STRUCTURES OF THE COMPOUNDS $Pr_2Co_{1.7}$ and $Nd_2Co_{1.7}$

Neutron experiments were carried out at the Oak Ridge Research

Reactor on powders of $Pr_2Co_{1.7}$ and $Nd_2Co_{1.7}$. Patterns were taken both

at room temperature, where the samples are in the paramagnetic state, and

at helium temperature where they are magnetically ordered. A measurement

of the intensities diffracted by a nickel powder placed in the same container

and the measurement of the absorption cross section of the samples permitted

putting all the measured intensities on an absolute scale. The experimental

absorption cross section, per formula unit are: $Pr_2Co_{1.7}$ = 73.4 barn and

$Nd_2Co_{1.7}$ = 132.1 barn.

ROOM TEMPERATURE MEASUREMENTS

At this temperature the compounds are magnetically disordered and

the diffracted intensities are of nuclear origin only:

$$I_{hk\ell} = pF_N^2 e^{-2w} \quad,$$

with

$$F_N = b_j \exp 2\pi i (hx_j + ky_j + \ell z_j)$$

p = multiplicity factor of the form (hkℓ)

$w = B \sin^2 \quad ^2$

B = temperature factor

b_j = Fermi length of the atom j .

Under such conditions, the neutron experiment should confirm the crystal

structure found in Chapter III. The comparison between observed and

calculated intensities is reported in Table I. For that calculation the following values were used:

$$b_{Pr} = 0.44 \ 10^{-12} cm$$

$$b_{Nd} = 0.72 \ 10^{-12} cm$$

$$b_{Co} = 0.25 \ 10^{-12} cm$$

$$B = 1.5 \ Å^2 \text{ as found by x-ray diffraction.}$$

One can see that the agreement is not very good. Particularly, with both compounds, the reflection (002) is observed with an intensity which is too high by a factor 2 (contribution of (200) is negligible). This suggests that a strong preferential orientation took place in the powders of both samples. Actually the grains have the shape of needles, and these needles tend to remain horizontal in the container. We have checked this point by an additional neutron experiment at room temperature on a $Pr_2Co_{1.7}$ powder consisting of coarser grains; the discrepancy for the (002) reflection was much stronger, which proved the role of preferential orientation.

HELIUM TEMPERATURE MEASUREMENTS

At 4.2^o K, the temperature of boiling helium, both $Pr_2Co_{1.7}$ and $Nd_2Co_{1.7}$ are magnetically ordered. As the neutrons used in that experiment were not polarized, the diffracted intensities are the sum of two contributions, one of nuclear and one of magnetic origin:

$$I_{hk\ell} = p \ (F_N^{\ 2} + g^2 F_M^{\ 2} \ e^{-2w}$$

$$F_M = 0.27 \ f_j \ m_j \ exp \ 2\pi i \ (hx_j + ky_j + \ell z_j)$$

$$m_j = \text{magnetic moment of the atom j (in } u_B)$$

f_j = magnetic form factor of the atom j

$g^2_{hk\ell}$ = geometrical factor characteristic of the direction of the moments in a collinear magnetic structure.

The neutron diffraction patterns obtained at that temperature, compared to room temperature patterns, show a strong magnetic contribution. Particularly, the strong increase of the (002) reflection suggests in both cases that the easy axis of the structure is not parallel to the c axis, a configuration which would imply $g^2_{(002)} = 0$. To minimize the errors due to the preferential orientation, we have deduced the magnetic intensities observed at room temperature, corrected with their temperature factor. These intensities fit well with a model of ferromagnetic arrangement of the moments where the easy axis is perpendicular to the c axis of the hexagonal structure. The best agreement is obtained for the following values of the moments:

$\underline{Pr}_2\underline{Co}_{1.7}$

$M_{Pr} = 2.65 \mu_B$

$M_{Co} = 0.70 \mu_B$

$\underline{Nd}_2\underline{Co}_{1.7}$
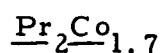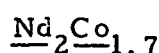
$M_{Nd} = 2.50 \mu_B$

$M_{Co} = 0.70 \mu_B$

This agreement between observed and calculated magnetic intensities is shown in Table II. Here again, the values observed for the (002) reflections are roughly two times too high, which was expected from the preferential orientation.

For this calculation, the form factors used for the rare-earth moments are the theoretical ones calculated by Blume et al[1], those used for cobalt were the ones measured by Moon[2].

The results obtained are surprising when compared to the results reported for $PrCo_2$[3] and $NdCo_2$[4]. The rare-earth moments are equivalent for the same kind of atom, but the cobalt moments are not. They were found to be $0.50 \, \mu_B$ in $PrCo_2$ and $0.80 \, \mu_B$ in $NdCo_2$. This variation may be explained by the crystal structure of the $R_2Co_{1.7}$ compounds where the Co-Co interactions, due to the short distance of $2.37 \, \overset{o}{A}$, should be much stronger than in RCo_2 compounds.

REFERENCES

1. M. Blume, A. J. Freeman, and R. E. Watson, $\underline{\text{J. Chem. Phys.}}$, 37:1245 (1962).

2. R. M. Moon, $\underline{\text{Phys. Rev.}}$, 136 A:195 (1964).

3. J. Schweizer, $\underline{\text{Phys. Lett.}}$, 24:739 (1967).

4. R. M. Moon, W. C. Koehler, and J. Farrell, $\underline{\text{J. Appl. Phys.}}$, 36:978 (1965).

TABLE I

OBSERVED AND CALCULATED NUCLEAR INTENSITIES
(IN BARNS)

h k ℓ	$Pr_2Co_{1.7}$		$Nd_2Co_{1.7}$	
	$pF_N^2 e^{-2w}{}_{obs}$	$pF_N^2 e^{-2w}{}_{cal}$	$pF_N^2 e^{-2w}{}_{obs}$	$pF_N^2 e^{-2w}{}_{cal}$
1 0 0	N. O.	0.001	0.57 ± 0.06	0.50
1 0 1	7.45 ± 0.21	6.39	20.51 ± 0.28	17.07
1 1 0	9.37 ± 0.67	8.98	18.84 ± 0.43	18.34
2 0 0 + 0 0 2	2.97 ± 0.70	1.29	7.60 ± 0.55	3.90
2 0 1 + 1 0 2	7.73 ± 0.40	7.48	22.15 ± 0.62	20.00
2 1 0 + 1 1 2	7.73 ± 0.55	6.82	22.31 ± 0.79	19.02

N. O. = Not Observed

TABLE II

OBSERVED AND CALCULATED MAGNETIC INTENSITIES
(IN BARNS)

h k ℓ	$Pr_2Co_{1.7}$		$Nd_2Co_{1.7}$	
	$pF_M{}^2obs$	$pF_M{}^2cal$	$pF_M{}^2obs$	$pF_M{}^2cal$
1 1 0	0.36 ±0.09	0.38	0.32 ±0.13	0.32
1 0 1	11.25 ±1.5	11.43	10.68 ±0.44	11.01
1 1 0	5.71 ±1.2	6.84	6.81 ±1.8	6.78
2 0 0	6.05 ±1.5	3.18 $\begin{cases} 0.39 \\ 2.79 \end{cases}$	5.13 ±1.8	3.19 $\begin{cases} 0.38 \\ 2.81 \end{cases}$
0 0 2				
2 0 1	12.31 ±1.0	10.52 $\begin{cases} 7.05 \\ 3.47 \end{cases}$	11.04 ±3.0	10.78 $\begin{cases} 7.23 \\ 3.55 \end{cases}$
1 0 2				
2 1 0	11.25 ±2.5	11.27 $\begin{cases} 0.77 \\ 10.50 \end{cases}$	15.17 ±5.0	11.64 $\begin{cases} 0.80 \\ 10.84 \end{cases}$
1 1 2				

CHAPTER V

DETERMINATION OF THE EASY AXIS OF MAGNETIZATION

BY MEANS OF X-RAY DIFFRACTION

DISCUSSION OF THE METHOD

The determination of the easy axis of magnetization of a ferro-magnetic or ferrimagnetic compound generally requires either magnetic measurements on an oriented single crystal or the use of neutron diffraction. When the magnetic anisotropy of the substance is high, however, a simpler method may be employed. This method involves x-ray diffraction measurements on powders pre-aligned in a magnetic field. The crystallo-graphic direction of the easy axis is deduced from the study of the orientation texture of the diffraction pattern. Strong anomalies are observed in diffraction patterns of pre-aligned powders obtained by the rotating crystal method as well as the Debye-Scherrer method. We shall briefly discuss these as an aid to a better understanding of the method used here.

If the sample is a powder without preferential orientation, the Bragg x-ray maxima are diffracted in cones, whose angles are at discrete values of $2\theta_{hkl}$. The recorded x-ray diffraction patterns have the general appearance of Figure 1.

If the sample is a single crystal rotating around an axis [u, v, w], the points (hkl) of the reciprocal lattice lie in a set of planes that are perpendicular to the vector [u, v, w]. As a consequence, during the rotation of the crystal, these planes cut the Ewald sphere along a discrete number of circles and the rotating crystal diffraction patterns

appear as shown in Figure 2. The Bragg reflections are located on discrete

horizontal lines. In particular, a reflection (hk$l$), lies on the nth line,

where uh + vk + wl = n.

DIFFRACTION BY A POWDER ALIGNED IN A MAGNETIC FIELD

The sample is a needle formed from a powder of the ferromagnetic

compound consisting, ideally, of single-crystal particles which have been

aligned and bonded with a cement in a magnetic field. The sample is

mounted on the goniometer of a rotating crystal camera with the long axis

of the needle parallel to the rotation axis. Each grain is now supposed to

be oriented with its easy axis of magnetization parallel to the axis of the

needle and therefore parallel to the axis of rotation. If the orientation

were perfect, the x-ray pattern obtained would be equivalent to that of a

single crystal rotating around its easy axis of magnetization. This is not

exactly the case; the magnetic alignment is not perfect and the x-ray

pattern is intermediate between a powder pattern and a rotating crystal

pattern. Debye-Scherrer lines are present, but they are very inhomogeneous

with strong intensity maxima occurring where the reflections would be if

the sample were a single crystal rotating around the same axis, as

illustrated in Figure 3. The stronger the magnetic anisotropy and the

stronger the magnetic field applied during the alignment process, the

stronger is the orientation texture of these lines. The analysis of the

texture indicates which crystalline axis of the grains is aligned on the

average with the long axis of the needle, which is the easy axis of

magnetization at the temperature at which the needle has been bonded.

CONCLUSIONS

a. This method is very convenient for determining the easy axis of magnetization at room temperature.

b. The magnetic field must be large enough to saturate the sample, i.e., to remove all magnetic domains except one in each grain. An insufficient field may align even single-crystal grains parallel to an axis different from the easy axis if two or more easy directions exist in the crystal. Even in a single-crystal grain with a unique easy axis, however, to which the total magnetic moment can only be parallel, the orienting mechanical torque moment exerted by the field may be too small unless the grain is nearly saturated.

c. This method works well only for materials with a strong magnetic crystal anisotropy. If the crystal anisotropy is not high, the shape anisotropy of the grains will also play a role in the alignment and may lead to wrong conclusions. The method is therefore very suitable for studying rare earth-cobalt-iron compounds because they are in general quite strongly anisotropic.

EXPERIMENTAL PROCEDURES

Freshly powdered, -200 mesh ($<78\mu m$), R_2Co_{17} and R_2Fe_{17} were premagnetized in a field of 26 kOe, mixed with an epoxy to form a thick paste and placed in a 6 kOe field to grow thin needles of oriented alloy particles. After the epoxy cured, needles were placed in a Weissenberg

camera and rotating crystal diffraction patterns were obtained.

Vanadium-filtered CrK_α radiation was employed. The direction of easy

magnetization was determined by qualitative evaluation of the texture

exhibited in the diffraction patterns.

RESULTS

The results of the magnetic easy axis determination are presented

in Table I for the R_2Co_{17} compounds and in Table II for R_2Fe_{17} compounds.
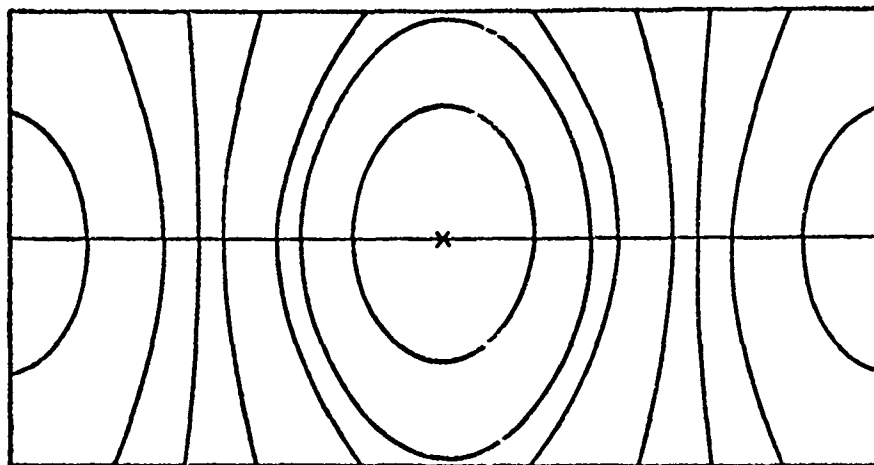
Figure 1. Rotating crystal method x-ray diffraction pattern of a crystalline powder without preferential orientation.
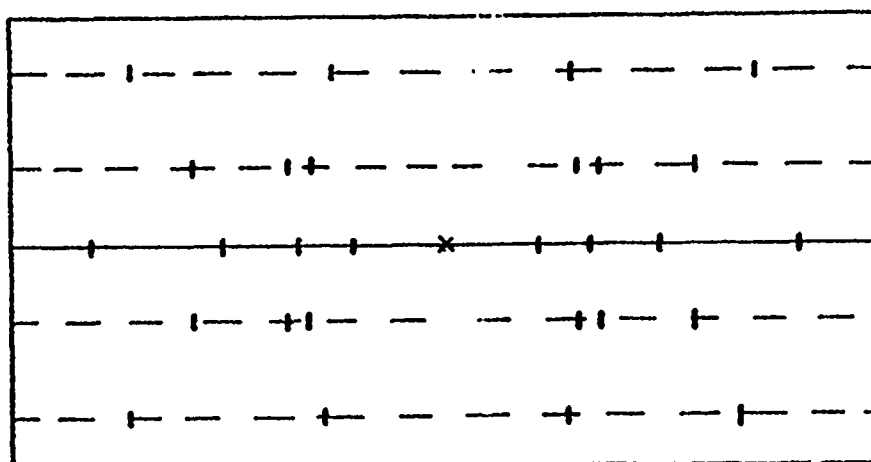
Figure 2. Rotating crystal method x-ray diffraction pattern of a single crystal aligned around a major axis.
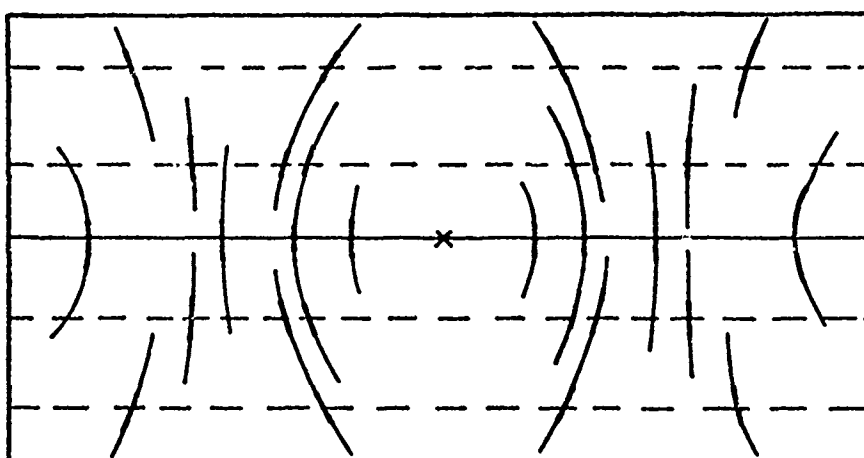
Figure 3. Rotating crystal method x-ray diffraction pattern of a crystalline powder with a strong preferential orientation around a major axis.

TABLE I

CRYSTAL ANISOTROPY OF R_2Co_{17}

COMPOUNDS AT ROOM TEMPERATURE

Compound	Crystal type	Easy direction
Ce_2Co_{17}	(*)	
Pr_2Co_{17}	rhomb.	in Basal Plane
Nd_2Co_{17}	rhomb.	
Sm_2Co_{17}	rhomb. (of 2)	c-axis
Gd_2Co_{17}	rhomb. (of 2)	
Tb_2Co_{17}	rhomb. (of 2)	in Basal Plane
Dy_2Co_{17}	mixture	
Ho_2Co_{17}	hexag.	
Er_2Co_{17}	hexag.	c-axis
Tm_2Co_{17}	hexag.	c-axis
Lu_2Co_{17}	hexag.	in Basal Plane
Y_2Co_{17}	rhomb. (of 2)	in Basal Plane

(*) Poor sample; contained $CeCo_5$

TABLE II

CRYSTAL ANISOTROPY OF R_2Fe_{17}

COMPOUNDS AT ROOM TEMPERATURE

Compound	Crystal Type	Easy Direction
Pr_2Fe_{17}	rhomb.	
Nd_2Fe_{17}	rhomb.	
Sm_2Fe_{17}	rhomb.	all in
Gd_2Fe_{17}	rhomb. (of 2)	Basal Plane
Tb_2Fe_{17}	misture	
Dy_2Fe_{17}	hexag.	
Ho_2Fe_{17}	hexag.	
Er_2Fe_{17}	hexag.	
Tm_2Fe_{17}	hexag.	
Y_2Fe_{17}	mixture	in Basal Plane

CHAPTER VI

CRYSTAL STRUCTURE OF THE COMPOUND $Ho_{12}Co_7$

In the phase diagram holmium-cobalt published by Buschow et al[1] only one of the compounds reported to exist was not yet described with regard to exact composition and crystal structure. It was labeled Ho_xCo by Buschow and corresponds to a composition of 37 at.% cobalt and 63 at.% holmium, with congruent melting behavior.

To undertake the study of the crystal structure of this compound we prepared, by arc melting, an alloy corresponding to the above composition and annealed it for 7 days at $750^{\circ}C$. After crushing the button, I was able to isolate a pseudo-cylindrical single crystal with a long axis of 0.157 mm and a diameter varying between 0.067 mm and 0.095 mm. An x-ray diffraction study was done on this crystal. The long axis appeared to be roughly the a axis of a monoclinic cell with the following lattice constants:

$$a = 9.30 \text{ Å} \qquad = 90^{\circ}$$
$$b = 13.85 \text{ Å} \qquad = 90^{\circ}$$
$$c = 11.16 \text{ Å} \qquad = 144^{\circ}$$

A pycnometric density evaluation was performed on a large piece of the compound, a value of 9.51 was found. The comparison between this density, the volume of the cell, and the composition led to the formula $Ho_{24}Co_{14}$ for one monoclinic cell.

We recorded on a Weissenberg camera 7 layers of x-ray reflections: $0k\ell$, $1k\ell$, $2k\ell$, $3k\ell$, $4k\ell$, $5k\ell$, and $6k\ell$. We used molybdenum characteristic

radiation, filtered by a zirconium foil, to bring the absorption to its lowest possible level. We estimated the intensities by comparison with a standard. The cylinder absorption correction has been performed with a calculated uR of 2.3, corresponding to an average diameter of 0.081 mm. To take into account the varying diameter of the cylinder we applied an empirical correction based on the comparison of several equivalent reflections in the plane $0k\ell$.

Systematic extinctions appeared for the reflections (hk0) where $k = 2n + 1$ and (00ℓ) for $\ell = 2n + 1$. These extinctions are characteristic of the space group $P2_1/b$ which has 4 equivalent positions for each site. From the composition $Ho_{24}Co_{12}$ one can deduce that there should be 6 sites for holmium and 3 sites for cobalt in general positions and one site for cobalt in a special position.

The measured intensities were treated with the usual procedure to obtain a sharpened Patterson function. To determine the location of the 6 holmium atoms of the asymmetrical unit, I took advantage of the Harker section of the Patterson function: 2 atoms deduced from each other by the operator 2_1 give an interaction in the plane $w = 1/2$. An implication of that Harker section[2] indicates the possible locations in the cell for the heavy atoms and I was left with the removal of the ambiguities. This removal was performed with the Patterson function by looking at the interaction of two possible atoms. After having located the 6 holmium atoms, the unknown cobalt atoms were revealed by inspection of a Fourier map based on the measured intensities together with the phases

due to the contribution of the holmium atoms only. Four atoms were found: 3 in general positions and one in the special position (1/2, 1/2, 0). A final least-squares refinement adjusted all the positions and the temperature coefficients; these values are given in Table I. Observed and calculated structure factors are reported in Table II. The agreement is very good and provides a confidence factor R = 8.1%.

REFERFNCES

1. K. H. J. Buschow and A. S. Van Der Goot, _J. Less-Common Metals_, 19:153 (1969).

2. M. J. Buerger, _Vector Space_, John Wiley, New York,

TABLE I

FINAL LEAST-SQUARES PARAMETERS OF $Ho_{12}Co_7$

Atom	set	x	y	z	$B(Å^2)$
Ho_I	e	0.1200(7)	0.4231 (4)	0.0704 (3)	1.50 (7)
Ho_{II}	e	0.4018(7)	0.0747 (4)	0.7027 (3)	1.44 (7)
Ho_{III}	e	0.0551(7)	0.1414 (4)	0.0719 (3)	1.54 (7)
Ho_{IV}	e	0.3121(7)	0.2725 (4)	0.7957 (3)	1.63 (7)
Ho_V	e	0.1787(7)	0.3390 (4)	0.3400 (3)	1.50 (7)
Ho_{VI}	e	0.4435(7)	0.2907 (4)	0.5050 (3)	1.59 (7)
Co_I	d	0.5	0.5	0.0	2.27(29)
Co_{II}	e	0.2131(24)	0.0615(24)	0.1943(11)	2.76(24)
Co_{III}	e	0.3220(20)	0.4164(12)	0.5896 (9)	1.60(18)
Co_{IV}	e	0.0240(25)	0.0536(16)	0.3365(13)	3.09(25)

4e: (x, y, z); $(\bar{x}, \bar{y}, \bar{z})$; $\bar{x}, 1/2-y, 1/2+z$); $(x, 1/2+y, 1/2-z)$.

2d: $(1/2, 1/2, 0)$, $(1/2, 0, 1/2)$.

TABLE II

$Ho_{12}Co_7$: OBSERVED AND CALCULATED STRUCTURE FACTORS

h	k	ℓ	F_{obs}	F_{cal}	h	k	ℓ	F_{obs}	F_{cal}	h	k	ℓ	F_{obs}	F_{cal}
0	2	0	90	74	0	9	4	74	89	0	4	9	178	202
0	4	0	160	141	0	10	4	92	99	0	5	9	-	4
0	6	0	237	225	0	1	5	144	152	0	6	9	70	63
0	8	0	162	174	0	2	5	154	158	0	7	9	171	179
0	10	0	95	65	0	3	5	-	38	0	8	9	79	80
0	2	1	118	120	0	4	5	330	359	0	10	9	106	103
0	3	1	554	483	0	5	5	119	120	0	0	10	205	244
0	4	1	108	108	0	6	5	124	127	0	1	10	70	76
0	5	1	192	183	0	7	5	-	17	0	2	10	66	61
0	6	1	96	82	0	8	5	150	146	0	3	10	127	135
0	7	1	163	157	0	9	5	-	30	0	4	10	146	168
0	8	1	77	60	0	0	6	143	148	0	5	10	-	23
0	9	1	-	16	0	1	6	90	85	0	6	10	188	196
0	10	1	-	199	0	2	6	202	209	0	7	10	79	75
0	11	1	79	76	0	3	6	403	409	0	1	11	-	42
0	1	2	37	34	0	4	6	203	217	0	2	11	-	35
0	2	2	45	45	0	5	6	-	8	0	3	11	100	100
0	3	2	544	473	0	6	6	133	140	0	4	11	121	112
0	4	2	70	73	0	7	6	68	61	0	5	11	63	43
0	5	2	112	112	0	8	6	55	62	0	6	11	113	106
0	6	2	124	117	0	9	6	79	87	0	0	12	138	153
0	7	2	117	108	0	1	7	146	164	0	1	12	-	11
0	8	2	-	31	0	2	7	102	114	0	2	12	-	24
0	9	2	117	112	0	3	7	130	136	0	3	12	-	26
0	10	2	73	88	0	4	7	-	18	0	4	12	111	103
0	1	3	66	59	0	5	7	80	92	0	5	12	-	14
0	2	3	126	134	0	6	7	93	88	0	6	12	126	126
0	3	3	43	43	0	7	7	325	339	0	2	13	-	38
0	4	3	-	28	0	8	7	-	49	0	3	13	204	204
0	5	3	94	92	0	0	8	353	395	0	4	13	157	150
0	6	3	173	171	0	1	8	130	146	0		14	260	285
0	7	3	306	308	0	2	8	120	146	0	1	14	-	7
0	8	3	117	103	0	3	8	355	376	0	2	14	-	42
0	9	3	156	156	0	4	8	176	190	0	3	14	137	127
0	0	4	107	107	0	5	8	83	80	0	1	15	85	89
0	1	4	555	540	0	6	8	149	164	1	-10	0	233	208
0	2	4	177	172	0	7	8	65	70	1	-8	0	220	180
0	3	4	-	21	0	8	8	40	35	1	-4	0	166	122
0	4	4	292	275	0	9	8	-	39	1	2	0	350	370
0	5	4	130	125	0	10	8	95	103	1	4	0	471	520
0	6	4	106	103	0	11	8	106	115	1	6	0	229	233
0	7	4	45	19	0	2	9	43	39	1	8	0	-	22
0	8	4	38	11	0	3	9	90	117	1	10	0	107	115

TABLE II (Cont)

Ho$_{12}$Co$_7$: OBSERVED AND CALCULATED STRUCTURE FACTORS

h	k	ℓ	F_{obs}	F_{cal}	h	k	ℓ	F_{obs}	F_{cal}	h	k	ℓ	F_{obs}	F_{cal}
1	-10	1	-	36	1	2	3	139	118	1	-10	6	129	122
1	-9	1	-	30	1	3	3	47	40	1	-9	6	-	30
1	-8	1	95	78	1	4	3	269	260	1	-8	6	157	150
1	-7	1	313	294	1	5	3	102	92	1	-7	6	153	127
1	-6	1	304	279	1	6	3	188	183	1	-6	6	87	84
1	-5	1	-	29	1	7	3	128	103	1	-5	6	92	83
1	-4	1	454	482	1	8	3	127	102	1	-4	6	371	384
1	1	1	50	28	1	-11	4	134	115	1	-3	6	-	47
1		1	217	284	1	-10	4	205	149	1	-2	6	-	50
1	3	1	145	120	1	-9	4	72	68	1	-1	6	-	34
1	4	1	-	20	1	-8	4	167	145	1	0	6	287	324
1	5	1	136	113	1	-7	4	303	254	1	1	6	185	177
1	6	1	177	173	1	-6	4	117	88	1	2	6	120	125
1	7	1	305	302	1	-5	4	126	107	1	4	6	269	272
1	-11	2	103	88	1	-4	4	61	45	1	5	6	-	44
1	-10	2	-	35	1	-3	4	357	370	1	6	6	-	6
1	-9	2	143	117	1	-2	4	276	258	1	-11	7	152	147
1	-8	2	136	112	1	-1	4	563	652	1	-9	7	108	106
1	-7	2	212	189	1	0	4	411	471	1	-8	7	-	16
1	-6	2	270	257	1	1	4	137	126	1	-7	7	65	50
1	-5	2	295	247	1	2	4	-	10	1	-6	7	80	72
1	-4	2	557	613	1	3	4	386	452	1	-5	7	104	82
1	-3	2	262	235	1	4	4	154	134	1	-4	7	292	287
1	-2	2	59	45	1	5	4	-	8	1	-3	7	291	294
1	0	2	100	92	1	6	4	61	56	1	-2	7	-	28
1	1	2	167	143	1	7	4	210	216	1	-1	7	383	427
1	2	2	249	240	1	-11	5	133	131	1	0	7	68	64
1	4	2	113	88	1	-10	5	-	7	1	1	7	231	204
1	5	2	87	57	1	-9	5	-	1	1	2	7	64	65
1	6	2	77	75	1	-8	5	135	137	1	3	7	72	87
1	7	2	-	17	1	-7	5	222	212	1	4	7	48	49
1	8	2	-	59	1	-6	5	-	40	1	-7	8	159	149
1		2	-	16	1	-5	5	84	79	1	-6	8	60	61
1		2	158	150	1	-4	5	249	224	1	-5	8	118	107
1		3	99	120	1	-3	5	-	21	1	-4	8	-	42
1			-	38	1	-2	5	66	60	1	-3	8	106	120
1		3	172	168	1	-1	5	164	170	1	-2	8	-	47
1			335	351	1	0	5	95	92	1	-1	8	203	195
1	-6	3	55	51	1	1	5	177	160	1	0	8	285	274
1	-5	3	302	327	1	2	5	152	162	1	1	8	117	109
1	-4	3	324	320	1	3	5	356	345	1	2	8	80	69
1	-3	3	546	566	1	4	5	181	162	1	3	8	-	12
1	-1	3	141	138	1	5	5	241	239	1	4	8	62	51
1	0	3	297	332	1	6	5	244	214	1	-8	9	91	73
1	1	3	141	128	1	-11	6	76	59	1	-7	9	-	40

TABLE II (Cont)

$Ho_{12}Co_7$: OBSERVED AND CALCULATED STRUCTURE FACTORS

h	k	l	F_{obs}	F_{cal}	h	k	l	F_{obs}	F_{cal}	h	k	l	F_{obs}	F_{cal}
1	-7	9	-	40	1	-2	12	-	65	2	2	2	341	387
1	-6	9	103	96	1	-1	12	148	128	2	3	2	203	230
1	-5	9	244	219	1	0	12	155	139	2	4	2	131	132
1	-4	9	-	14	1	1	12	74	52	2	5	2	-	51
1	-3	9	85	105	1	2	12	189	178	2	6	2	-	62
1	-2	9	-	22	1	-1	13	152	126	2	7	2	192	182
1	-1	9	85	90	1	-7	13	185	171	2	-11	3	-	21
1	0	9	85	97	1	-7	14	150	132	2	-10	3	104	96
1	1	9	-	2	2	-10	0	460	429	2	-9	3	77	80
1	2	9	192	196	2	-8	0	81	69	2	-8	3	54	55
1	3	9	282	299	2	-6	0	185	160	2	-7	3	-	12
1	4	9	106	84	2	-4	0	502	477	2	-6	3	-	29
1	-10	10	144	138	2	0	0	145	117	2	-5	3	149	124
1	-9	10	-	22	2	2	0	212	203	2	-4	3	175	155
1	-8	10	171	180	2	4	0	173	210	2	-3	3	487	489
1	-7	10	151	163	2	6	0	-	3	2	-2	3	117	107
1	-6	10	-	10	2	-11	1	203	150	2	-1	3	554	594
1	-5	10	96	98	2	-10	1	-	64	2	0	3	176	179
1	-4	10	58	79	2	-9	1	-	37	2	1	3	96	88
1	-3	10	187	194	2	-8	1	448	398	2	2	3	261	239
1	-2	10	128	131	2	-7	1	123	95	2	3	3	48	57
1	-1	10	134	143	2	-6	1	71	49	2	4	3	207	223
1	0	10	370	358	2	-5	1	358	312	2	-11	4	166	136
1	2	10	-	36	2	-4	1	-	22	2	-10	4	166	137
1	3	10	-	2	2	-1	1	204	199	2	-9	4	71	52
1	4	10	120	92	2	0	1	715	708	2	-8	4	106	96
1	-10	11	204	182	2	1	1	285	278	2	-7	4	134	122
1	-9	11	-	2	2	2	1	-	38	2	-6	4	216	207
1	-8	11	79	78	2	3	1	365	373	2	-5	4	108	96
1	-7	11	124	105	2	4	1	148	158	2	-4	4	238	248
1	-6	11	-	20	2	5	1	-	10	2	-3	4	220	237
1	-5	11	-	62	2	6	1	203	194	2	-2	4	-	2
1	-4	11	134	126	2	-11	2	-	14	2	-1	4	120	117
1	-3	11	66	59	2	-10	2	-	44	2	0	4	155	160
1	-2	11	-	40	2	-9	2	185	171	2	1	4	-	24
1	-1	11	-	44	2	-8	2	142	124	2	2	4	125	116
1	0	11	350	332	2	-7	2	408	375	2	3	4	98	74
1	1	11	-	27	2	-6	2	75	55	2	4	4	168	167
1	2	11	119	112	2	-5	2	410	367	2	5	4	71	50
1	3	11	-	31	2	-4	2	61	2	2	-9	5	72	66
1	4	11	176	175	2	-3	2	164	156	2	-8	5	-	4
1	-7	12	128	119	2	-2	2	99	100	2	-7	5	158	154
1	-6	12	-	48	2	-1	2	279	317	2	-6	5	147	133
1	-5	12	-	35	2	0	2	405	414	2	-5	5	295	287
1	-4	12	177	181	2	1	2	180	172	2	-4	5	-	9
1	-3	12	170	166										

TABLE II (Cont)

$Ho_{12}Co_7$: OBSERVED AND CALCULATED STRUCTURE FACTORS

h	k	l	F_{obs}	F_{cal}	h	k	l	F_{obs}	F_{cal}	h	k	l	F_{obs}	F_{cal}
2	-3	5	100	89	2	-5	8	152	149	3	-12	0	201	205
2	-2	5	123	130	2	-4	8	332	361	3	-10	0	-	41
2	-1	5	223	237	2	-3	8	111	112	3	-2	0	142	124
2	0	5	145	137	2	-2	8	-	5	3	0	0	-	22
2	1	5	-	35	2	-1	8	164	144	3	2	0	159	151
2	2	5	-	48	2	0	8	37	89	3	-4	1	255	260
2	3	5	83	83	2	1	8	108	95	3	-3	1	463	453
2	4	5	-	38	2	2	8	200	202	3	-2	1	488	446
2	5	5	94	63	2	3	8	-	63	3	-1	1	108	84
2	6	5	168	153	2	4	8	-	29	3	0	1	-	25
2	7	5	172	150	2	5	8	-	36	3	1	1	104	92
2	-10	6	201	169	2	6	8	98	93	3	2	1	107	87
2	-9	6	-	2	2	-8	9	193	182	3	3	1	97	90
2	-8	6	336	320	2	-7	9	-	21	3	4	1	82	78
2	-7	6	287	329	2	-6	9	100	88	3	-7	2	84	75
2	-6	6	88	82	2	-5	9	93	90	3	-6	2	91	91
2	-5	6	-	9	2	-4	9	-	19	3	-5	2	380	351
2	-4	6	351	365	2	-3	9	146	142	3	-4	2	353	378
2	-3	6	74	69	2	-3	9	169	162	3	-3	2	153	163
2	-2	6	-	31	2	-1	9	72	84	3	-2	2	123	109
2	-1	6	337	367	2	0	9	292	304	3	-1	2	89	74
2	0	6	-	18	2	1	9	-	38	3	0	2	218	196
2	1	6	-	20	2	2	9	-	23	3	1	2	69	67
2	2	6	86	97	2	3	9	-	52	3	2	2	196	196
2	3	6	-	43	2	6	9	216	220	3	3	2	-	7
2	4	6	-	64	2	-10	10	110	103	3	4	2	110	111
2	6	6	217	202	2	-9	10	97	94	3	5	2	187	194
2	-11	7	336	305	2	-8	10	82	80	3	6	2	223	228
2	-10	7	-	14	2	-7	10	148	128	3	-13	3	157	155
2	-9	7	88	96	2	-6	10	189	187	3	-12	3	124	123
2	-8	7	126	117	2	-5	10	202	204	3	-11	3	199	216
2	-7	7	228	254	2	-4	10	197	214	3	-10	3	98	102
2	-6	7	-	11	2	-3	10	150	157	3	-9	3	161	154
2	-5	7	-	8	2	-2	10	-	48	3	-8	3	149	146
2	-4	7	-	44	2	-1	10	-	31	3	-7	3	59	54
2	-3	7	408	426	2	0	10	-	32	3	-6	3	-	40
2	-2	7	98	103	2	-6	11	153	139	3	-5	3	245	229
2	-1	7	154	163	2	-5	11	110	108	3	-4	3	524	554
2	0	7	210	205	2	-4	11	137	143	3	-3	3	232	232
2	1	7	-	52	2	-3	11	68	62	3	-2	3	81	73
2	2	7	-	5	2	-2	11	141	142	3	-1	3	281	261
2	3	7	438	465	2	-5	12	127	111	3	0	3	363	336
2	-8	8	186	176	2	-4	12	165	163	3	1	3	252	218
2	-7	8	174	180	2	-3	12	151	142	3	2	3	320	323
2	-6	8	109	84	2	-4	14	181	200	3	3	3	266	251

TABLE II (Cont)

Ho$_{12}$Co$_7$: OBSERVED AND CALCULATED STRUCTURE FACTORS

h	k	l	F$_{obs}$	F$_{cal}$	h	k	l	F$_{obs}$	F$_{cal}$	h	k	l	F$_{obs}$	F$_{cal}$
3	-11	4	242	280	3	-9	7	135	136	3	-5	11	113	114
3	-10	4	186	190	3	-8	7	-	10	3	-4	11	168	181
3	-9	4	92	87	3	-7	7	73	74	3	-3	11	71	90
3	-8	4	-	16	3	-6	7	-	26	3	-2	11	90	86
3	-7	4	461	443	3	-5	7	197	209	3	-1	11	-	31
3	-6	4	-	45	3	-4	7	181	180	3	0	11	22	208
3	-5	4	-	27	3	-3	7	201	181	3	1	11	74	68
3	-4	4	144	146	3	-2	7	73	89	3	2	11	221	235
3	-3	4	-	57	3	-1	7	263	283	3	-8	12	179	188
3	-2	4	175	168	3	-12	8	117	132	3	-7	12	-	49
3	-1	4	142	141	3	-11	8	-	59	3	-6	12	145	147
3	0	4	-	6	3	-10	8	108	116	3	-5	12	149	156
3	1	4	-	12	3	-9	8	-	3	3	-4	12	121	109
3	2	4	-	7	3	-6	8	77	67	3	-3	12	-	2
3	3	4	223	211	3	-5	8	95	107	3	0	12	166	151
3	4	4	162	144	3	-4	8	56	81	3	-3	13	217	219
3	5	4	137	134	3	-3	8	174	193	4	-14	0	195	155
3	-11	5	153	163	3	-2	8	-	8	4	-12	0	249	194
3	-10	5	120	108	3	-1	8	203	222	4	-10	0	-	55
3	-9	5	132	142	3	0	8	85	123	4	-6	0	134	110
3	-8	5	166	178	3	1	8	-	19	4	-4	0	354	325
3	-7	5	375	343	3	2	8	199	209	4	-2	0	100	76
3	-6	5	-	38	3	-8	9	191	220	4	0	6	178	164
3	-5	5	255	243	3	-7	9	172	176	4	2	0	217	195
3	-4	5	336	333	3	-6	9	-	32	4	4	0	267	270
3	-3	5	-	31	3	-5	9	-	18	4	6	0	166	149
3	-2	5	-	29	3	-4	9	-	15	4	-6	1	217	167
3	-1	5	661	634	3	-3	9	-	24	4	-5	1	356	373
3	0	5	157	187	3	-2	9	180	196	4	-4	1	443	405
3	1	5	106	100	3	-1	9	199	208	4	-3	1	157	169
3	2	5	-	3	3	0	9	72	90	4	-2	1	-	9
3	3	5	240	228	3	1	9	169	193	4	-1	1	481	484
3	-10	6	124	141	3	-10	10	139	142	4	0	1	142	131
3	-9	6	84	95	3	-7	10	104	111	4	1	1	173	182
3	-8	6	61	66	3	-6	10	75	74	4	2	1	299	301
3	-7	6	-	22	3	-5	10	209	217	4	-8	2	248	221
3	-6	6	241	253	3	-4	10	129	133	4	-7	2	76	59
3	-5	6	-	12	3	-3	10	-	36	4	-6	2	346	369
3	-4	6	367	375	3	-1	10	124	133	4	-5	2	356	366
3	-3	6	117	125	3	0	10	127	131	4	-4	2	170	131
3	-2	6	82	98	3	-10	11	109	120	4	-3	2	180	178
3	-1	6	209	238	3	-9	11	-	48	4	-2	2	195	174
3	0	6	199	198	3	-8	11	223	213	4	-1	2	86	82
3	1	6	-	74	3	-7	11	-	13	4	0	2	-	34
3	2	6	113	137	3	-6	11	-	63	4	1	2	131	141

TABLE II (Cont)

Ho$_{12}$Co$_7$: OBSERVED AND CALCULATED STRUCTURE FACTORS

h	k	ℓ	F_{obs}	F_{cal}	h	k	ℓ	F_{obs}	F_{cal}	h	k	ℓ	F_{obs}	F_{cal}
4	2	2	152	149	4	-6	6	43	47	5	0	1	-	32
4	3	2	138	135	4	-5	6	261	291	5	1	1	71	76
4	-13	3	174	171	4	-4	6	88	79	5	2	1	144	119
4	-12	3	90	88	4	-3	6	-	43	5	-8	2	460	409
4	-11	3	149	171	4	-2	6	182	211	5	-7	2	184	110
4	-10	3	93	95	4	-1	6	-	41	5	-6	2	187	207
4	-9	3	117	115	4	0	6	104	115	5	-5	2	351	365
4	-8	3	212	207	4	3	6	196	182	5	-4	2	389	405
4	-7	3	61	46	4	-10	7	148	161	5	-3	2	143	137
4	-6	3	131	117	4	-9	7	-	30	5	-2	2	307	271
4	-5	3	147	153	4	-8	7	-	40	5	-1	2	132	127
4	-4	3	-	19	4	-7	7	286	317	5	0	2	149	151
4	-3	3	81	104	4	-6	7	170	173	5	1	2	-	31
4	-2	3	275	253	4	-5	7	99	105	5	2	2	154	161
4	-1	3	122	110	4	-4	7	92	87	5	-11	3	99	101
4	0	3	144	144	4	-3	7	117	121	5	-10	3	-	27
4	1	3	-	33	4	-2	7	-	4	5	-9	3	134	132
4	-12	4	116	115	4	-1	7	230	263	5	-8	3	364	371
4	-11	4	49	58	4	0	7	-	40	5	-7	3	273	264
4	-10	4	106	105	4	1	7	179	159	5	-6	3	-	9
4	-9	4	404	376	4	2	7	129	124	5	-5	3	111	108
4	-8	4	156	179	4	-11	8	205	199	5	-4	3	254	278
4	-7	4	219	236	4	-10	8	54	68	5	-3	3	235	251
4	-6	4	182	195	4	-9	8	117	131	5	-2	3	128	114
4	-5	4	99	91	4	-8	8	446	404	5	0	3	-	20
4	-4	4	-	3	4	-7	8	126	149	5	1	3	153	149
4	-3	4	116	129	4	-6	8	145	155	5	-15	4	118	127
4	-2	4	70	97	4	-5	8	165	177	5	-14	4	-	49
4	0	4	-	33	4	-4	8	-	8	5	-13	3	86	93
4	1	4	140	144	4	-3	8	117	94	5	-12	4	-	31
4	-9	5	249	237	4	-9	9	144	161	5	-11	4	232	230
4	-8	5	148	135	4	-8	9	95	85	5	-10	4	85	74
4	-7	5	198	198	4	-7	9	77	68	5	-9	4	324	316
4	-6	5	211	240	4	-6	9	96	95	5	-8	4	54	62
4	-5	5	174	215	4	-5	9	305	298	5	-7	4	146	139
4	-4	5	354	311	4	-4	9	346	369	5	-6	4	245	276
4	-3	5	200	197	4	-3	9	160	171	5	-5	4	264	298
4	-2	5	153	161	5	-4	0	-	14	5	-4	4	75	66
4	-1	5	231	276	5	-2	0	448	383	5	-3	4	-	2
4	0	5	196	200	5	0	0	-	15	5	-2	4	89	88
4	1	5	196	203	5	2	0	169	127	5	-1	4	346	332
4	-11	6	234	246	5	-5	1	234	226	5	0	4	-	13
4	-10	6	-	48	5	-4	1	89	78	5	1	4	-	16
4	-9	6	-	19	5	-3	1	90	75	5	2	4	139	144
4	-8	6	192	200	5	-2	1	163	165	5	3	4	181	172
4	-7	6	-	12	5	-1	1	-	38	5	-15	5	167	172

TABLE II (Cont)

$Ho_{12}Co_7$: OBSERVED AND CALCULATED STRUCTURE FACTORS

h	k	ℓ	F_{obs}	F_{cal}	h	k	ℓ	F_{obs}	F_{cal}	h	k	ℓ	F_{obs}	F_{cal}
5	-13	5	135	134	5	-9	8	132	141	6	-9	2	94	106
5	-12	5	-	33	5	-8	8	137	.25	6	-8	2	65	58
5	-11	5	282	274	5	-7	8	-	20	6	-7	2	81	90
5	-10	5	-	2	5	-6	8	143	136	6	-6	2	123	154
5	-9	5	151	168	5	-5	8	62	62	6	-5	2	210	221
5	-8	5	89	90	5	-4	8	114	103	6	-4	2	180	163
5	-7	5	102	107	5	-2	8	296	306	6	-3	2	-	47
5	-6	5	225	249	5	1	8	188	177	6	-2	2	279	301
5	-5	5	234	253	5	-12	9	95	103	6	-1	2	312	317
4	-4	5	79	100	5	-11	9	142	147	6	0	2	102	78
5	-3	5	-	4	5	-10	9	-	1	6	1	2	-	6
5	-2	5	158	181	5	-9	9	114	101	6	-14	3	-	40
5	-1	5	206	217	5	-8	9	-	59	6	-13	3	192	198
5	0	5	105	66	5	-7	9	-	41	6	-12	3	212	206
5	1	5	116	90	5	-6	9	147	130	6	-11	3	106	96
5	-16	6	194	173	5	-5	9	238	239	6	-10	3	-	0
5	-15	6	-	16	5	-4	9	-	37	6	-9	3	109	110
5	-14	6	123	121	5	-3	9	149	141	6	-8	3	116	137
5	-13	6	-	64	5	-2	9	-	43	6	-7	3	-	15
5	-12	6	142	180	5	-1	9	229	217	6	-6	3	183	215
5	-11	6	97	112	5	-11	10	140	146	6	-5	3	-	0
5	-10	6	162	165	5	-8	10	140	151	6	-4	3	198	199
5	-9	6	57	62	5	-6	10	146	158	6	-3	3	-	17
5	-8	6	-	27	5	-8	11	283	283	6	-2	3	-	55
5	-7	6	111	124	5	-4	11	205	190	6	0	3	-	4
5	-6	6	82	110	5	-8	12	199	209	6	1	3	192	220
5	-5	6	251	273	6	-6	0	501	396	6	-13	4	49	67
5	-4	6	94	121	5	-4	0	225	212	6	-12	4	-	60
5	-2	6	-	22	6	-2	0	245	231	6	-11	4	-	35
5	-2	6	96	101	6	0	0	-	5	6	-10	4	63	72
5	-1	6	81	85	6	2	0	201	219	6	-9	4	229	228
5	0	6	191	211	6	-8	1	462	426	6	-8	4	73	46
5	1	6	181	161	6	-7	1	-	6	6	-7	4	95	76
5	-13	7	161	157	6	-6	1	89	82	6	-6	4	133	155
5	-12	7	87	94	6	-5	1	324	315	6	-5	4	150	164
5	-11	7	-	27	6	-4	1	148	153	6	-4	4	-	75
5	-10	7	-	27	6	-3	1	124	101	6	-3	4	127	124
5	-9	7	176	164	6	-2	1	147	147	6	-1	4	-	31
5	-8	7	-	23	6	-1	1	67	78	6	0	4	95	90
5	-7	7	120	128	6	0	1	88	82	6	1	4	136	146
5	-6	7	-	56	6	1	1	-	27	6	-14	5	86	101
5	-5	7	70	64	6	-16	2	187	215	6	-13	5	-	16
5	-4	7	-	28	6	-15	2	132	172	6	-12	5	129	125
5	-11	8	118	111	6	-11	2	116	115	6	-11	5	168	174
5	-10	8	-	14	6	-10	2	81	61	6	-10	5	112	118

TABLE II (concluded)

$Ho_{12}Co_7$: OBSERVED AND CALCULATED STRUCTURE FACTORS

h	k	l	F_{obs}	F_{cal}	h	k	l	F_{obs}	F_{cal}
6	-9	5	376	401	6	-7	8	165	140
6	-8	5	149	149	6	-6	8	-	34
6	-7	5	187	214	6	-5	8	-	34
6	-6	5	114	100	6	-4	8	239	260
6	-5	5	115	102	6	-3	8	-	49
6	-3	5	-	15	6	-2	8	-	22
6	-2	5	132	134	6	-14	9	90	101
6	-1	5	-	9	6	-13	9	-	48
6	0	5	56	38	6	-12	9	-	23
6	1	5	71	49	6	-11	9	-	14
6	-15	6	185	203	6	-10	9	-	1
6	-14	6	115	106	6	-9	9	177	170
6	-13	6	-	24	6	-8	9	303	280
6	-12	6	175	167	6	-7	9	61	54
6	-11	6	-	4	6	-6	9	-	27
6	-10	6	44	51	6	-5	9	82	89
6	-9	6	211	217	6	-4	9	-	29
6	-8	6	44	62	6	-2	9	121	149
6	-7	6	118	144	6	-13	10	93	114
6	-6	6	397	396	6	-12	10	91	105
6	-5	6	-	8	6	-11	10	82	79
6	-4	6	156	153	6	-9	10	-	18
6	-3	6	-	62	6	-9	10	-	17
6	-2	6	128	123	6	-7	10	92	69
6	-1	6	200	195	6	-6	10	132	99
6	-12	7	-	4	6	-5	10	170	173
6	-11	7	128	112	6	-4	10	-	7
6	-10	7	99	90	6	-3	10	-	26
6	-9	7	292	296	6	-2	10	-	60
6	-8	7	79	74	6	-1	10	89	112
6	-7	7	150	134	6	-12	11	104	112
6	-6	7	-	20	6	-11	11	-	84
6	-5	7	376	351	6	-10	11	112	123
6	-4	7	-	36	6	-7	11	-	4
6	-3	7	160	170	6	-6	11	148	131
6	-2	7	66	20	6	-5	11	-	64
6	-15	8	92	99	6	-4	11	163	153
6	-14	8	-	16	6	-12	12	125	141
6	-13	8	-	47	6	-11	12	-	52
6	-12	8	227	253	6	-10	12	-	21
6	-11	8	63	69	6	-9	12	-	20
6	-10	8	-	56	6	-7	12	-	62
6	-9	8	112	101	6	-6	12	-	6
6	-8	8	-	6	6	-8	13	132	130

APPENDIX

During the contract period, January 1, 1971 through December 31, 1971, the following listed alloys were prepared by the University of Dayton Research Institute. The list gives the name of the person who ordered the alloy, the date ordered, the alloy number, the composition of the alloy, the heat treatment, and the amount prepared.

Name of Requestor	Date Ordered	Alloy (AR) Number	Composition	Heat Treatment (hrs/°C)	Amount Prepared (Grams)
Schweizer	1-21-71	739	40 a/o Y - 60 a/o Co	None	20
Evans	1-26-71	741	$PrCo_5$	None	30
Evans	1-26-71	742	$PrCo_4Cu_1$	None	30
Evans	1-26-71	743	$PrCo_{3.5}Cu_{1.5}$	None	30
Evans	1-26-71	744	$PrCo_3Cu_2$	None	30
Evans	1-27-71	745	$PrCu_5$	None	30
Evans	1-27-71	746	$PrCo_3Mn_2$	None	30
Evans	1-28-71	747	$SmCo_3Cu_2$	None	30
Evans	1-28-71	748	$SmCo_{3.5}Cu_{1.5}$	None	30
Evans	1-28-71	749	$SmCu_5$	None	30
Schweizer	2-01-71	751	74 w/o Pr- 26 w/o Co	None	10
Schweizer	2-01-71	752	76 w/o Pr- 24 w/o Co	None	10
Schweizer	2-01-71		$Er_{.18}Ni_{.82}$	48 hrs at 100°	10
Schweizer	2-01-71		$Er_{.21}Ni_{.79}$	48 hrs at 100°	10

Name of Requestor	Date Ordered	Alloy (AR) Number	Composition	Heat Treatment (hrs/°C)	Amount Prepared (Grams)
Schweizer	3-02-71	781	75.2 w/o Sm-24.8 w/o Co	None	15
Schweizer	3-02-71	782	73.8 w/o S 26.2 a/o Co	None	15
Schweizer	3-02-71	783	74.4 w/o Sm-25.6 w/o Co	None	10
Schweizer	3-09-71	790	Pr_2Co_7	None	10
Schweizer	3-09-71	791	$PrCo_4$	None	10
Schweizer	3-09-71	792	$PrCo_5$	None	10
Evans	3-10-71	793	$PrCo_5$	None	25
Evans	3-10-71	794	$PrCo_4Cu_1$	None	25
Evans	3-10-71	795	$PrCo_{3.5}Cu_{1.5}$	None	25
Evans	3-10-71	796	$PrCo_3Cu_2$	None	25
Evans	3-10-71	797	$SmCo_{3.5}Cu_{1.5}$	None	25
Evans	3-10-71	798	$SmCo_3Cu_2$	None	25
Evans	3-12-71	799	$PrCo_3Mn_2$	None	25
Schweizer	5-11-71	862	18.1 a/o Pr-81.9 a/o Co	None	20
Schweizer	5-12-71	863	19.8 a/o Pr-80.2 a/o Co	None	20
Schweizer	5-12-71	864	21.2 a/o Pr-78.8 a/o Co	None	20
Evans	5-13-71	865	$Nb_8(Al_{.75}Ge_{.25})_{.20}$	None	10
Schweizer	5-21-71	879	69.2 a/o Sm-30.8 a/o Co	60 hrs at 550°	50
Schweizer	5-21-71	880	75 a/o Sm-25 a/o Co	60 hrs at 550°	50
Evans	5-24-71	881	$Nb_8(Al_{.75}Ge_{.25})_{.20}$	None	10
Schweizer	5-27-71	884	74.4 w/o Nd-25.6 w/o Co	80 hrs at 500°	30
Schweizer	5-27-71	885	74 w/o Pr-26 w/o Co	80 hrs at 500°	40

Name of Requestor	Date Ordered	Alloy (AR) Number	Composition	Heat Treatment (hrs/^{o}C)	Amount Prepared (Grams)
Garrett	5-28-71	886	19.4 a/o Y-80.6 a/o Co	None	250
Schweizer	6-16-71	891	$Pr_2(Co_8Fe_2)_{1.7}$	48 hrs at 500°	30
Garrett	7-28-71	919	$NdCo_{4.85}Fe_{.15}$ Fe-57	None	25
Garrett	8-06-71	921	V A/3	None	.7
Garrett	8-10-71	924	$Nd_{.9}Gd_{.1}Co_5$	24 hrs at 1100°	25
Garrett	8-10-71	925	$Nd_{.7}Gd_{.3}Co_5$	24 hrs at 1100°	25
Garrett	8-10-71	926	$Nd_{.5}Gd_{.5}Co_5$	24 hrs at 1100°	25
Schweizer	8-24-71	929	$La_2Co_{1.7}$	60 hrs at 530°	25
Schweizer	8-26-71	934	$Ce_{24}Co_{11}$	None	20
Schweizer	8-26-71	935	Ce_7Ni_3	None	20
Schweizer	9-10-71	938	$Gd_{24}Co_{14}$	None	5
Schweizer	9-10-71	939	$Y_{24}Co_{14}$	None	5
Schweizer	9-10-71	940	$Dy_{24}Co_{14}$	None	5
Schweizer	9-10-71	941	$Er_{24}Co_{14}$	None	5
Schweizer	9-10-71	942	$Tb_{24}Co_{14}$	None	5
Garrett	9-14-71	943	$PrCo_5$	None	25
Garrett	9-14-71	944	$NdCo_5$	None	25
Garrett	9-14-71	945	YCo_5	None	25
Garrett	9-14-71	946	$SmCo_5$	None	25
Evans	12-07-71	986	$PrCo_{35}Cu_{1.5}$	None	40
Evans	12-07-71	987	$SmCo_{3.5}Cu_{1.5}$	None	27
VonRichter	1-18-72	1002	$Nd_{.8}Gd_2Co_5$	96 hrs at 1240°	25

Name of Requestor	Date Ordered	Alloy (AR) Number	Composition	Heat Treatment (hrs/$^{\circ}$C)	Amount Prepared (Grams)
VonRichter	1-18-72	1003	$Nd_{.6}Gd_{.4}Co_5$	96 hrs at 1240°	25
VonRichter	1-18-72	1004	$Nd_{.4}Gd_{.6}Co_5$	96 hrs at 1240°	25
VonRichter	1-18-72	1005	$Nd_{.9}Y_{.1}Co_5$	96 hrs at 1240°	25
VonRichter	1-18-72	1006	$Nd_{.8}Y_{.2}Co_5$	96 hrs at 1240°	25
VonRichter	1-18-72	1007	$Nd_{.7}Y_{.3}Co_5$	96 hrs at 1240°	25
VonRichter	1-18-72	1008	$Nd_{.6}Y_{.4}Co_5$	96 hrs at 1240°	25
VonRichter	1-18-72	1009	$Nd_{.5}Y_{.5}Co_5$	96 hrs at 1240°	25